



**HAL**  
open science

## **Laminin-binding integrins are essential for the maintenance of functional mammary secretory epithelium in lactation**

Mathilde Romagnoli, Laura Bresson, Amandine Di-Cicco, Maria Pérez-Lanzón, Patricia Legoix, Sylvain Baulande, Pierre de La Grange, Adèle de Arcangelis, Elisabeth Georges-Labouesse, Arnoud Sonnenberg, et al.

### ► To cite this version:

Mathilde Romagnoli, Laura Bresson, Amandine Di-Cicco, Maria Pérez-Lanzón, Patricia Legoix, et al.. Laminin-binding integrins are essential for the maintenance of functional mammary secretory epithelium in lactation. *Development* (Cambridge, England), In press, 10.1242/dev.181552. hal-02472516

**HAL Id: hal-02472516**

**<https://hal.sorbonne-universite.fr/hal-02472516>**

Submitted on 10 Feb 2020

**HAL** is a multi-disciplinary open access archive for the deposit and dissemination of scientific research documents, whether they are published or not. The documents may come from teaching and research institutions in France or abroad, or from public or private research centers.

L'archive ouverte pluridisciplinaire **HAL**, est destinée au dépôt et à la diffusion de documents scientifiques de niveau recherche, publiés ou non, émanant des établissements d'enseignement et de recherche français ou étrangers, des laboratoires publics ou privés.

## **Laminin-binding integrins are essential for the maintenance of functional mammary secretory epithelium in lactation**

Mathilde Romagnoli<sup>1,2,3</sup>, Laura Bresson<sup>1,2,3</sup>, Amandine Di-Cicco<sup>1,2</sup>, María Pérez-Lanzón<sup>1,2,4</sup>, Patricia Legoix<sup>5</sup>, Sylvain Baulande<sup>5</sup>, Pierre de la Grange<sup>6</sup>, Adèle De Arcangelis<sup>7</sup>, Elisabeth Georges-Labouesse<sup>7</sup>, Arnoud Sonnenberg<sup>8</sup>, Marie-Ange Deugnier<sup>1,2,9</sup>, Marina A. Glukhova<sup>1,2,9</sup>, Marisa M. Faraldo<sup>1,2,9,10</sup>

<sup>1</sup>Institut Curie, PSL Research University, CNRS, UMR144, F-75005 Paris, France.

<sup>2</sup>Sorbonne Universités, UPMC Univ Paris 06, F-75005 Paris, France.

<sup>3</sup>Present address: Institut de Recherche Servier, F-78290 Croissy, France

<sup>4</sup>Present address: Centre de Recherche des Cordeliers, INSERM, F-75006 Paris, France. Faculty of Medicine, Paris Sud/Paris XI University, Le Kremlin-Bicêtre, France

<sup>5</sup>Institut Curie Genomics of Excellence (ICGex) Platform, Institut Curie, Paris, France

<sup>6</sup>GenoSplice Technology, F-75005 Paris, France

<sup>7</sup>Institut de Génétique et de Biologie Moléculaire et Cellulaire, CNRS UMR7104/INSERM U964/ULP, F-67404 Illkirch, France.

<sup>8</sup>Division of Cell Biology, The Netherlands Cancer Institute, 1066 CX Amsterdam, The Netherlands.

<sup>9</sup>Inserm, Paris, F-75013, Paris, France

<sup>10</sup>**Corresponding author:** Marisa M. Faraldo, Institut Curie, PSL Research University, CNRS, UMR144, 26 rue d'Ulm, F-75005, Paris, France.

Phone: +33(0)156246332; Fax: +33(0)156246349; e-mail: [maria-luisa.martin-faraldo@curie.fr](mailto:maria-luisa.martin-faraldo@curie.fr)

**Running title:** integrins in mammary gland

**Key words:** mammary gland; Cre-Lox gene deletion; integrin; laminin; differentiation;  
p53

## ABSTRACT

Integrin dimers  $\alpha3/\beta1$ ,  $\alpha6/\beta1$  and  $\alpha6/\beta4$  are the mammary epithelial cell receptors for laminins, which are major components of the mammary basement membrane. The roles of specific basement membrane components and their integrin receptors in the regulation of functional gland development have not been analyzed in detail. To investigate the functions of laminin-binding integrins, we obtained mutant mice with mammary luminal cell-specific deficiencies of the  $\alpha3$  and  $\alpha6$  integrin chains generated by the Cre-Lox approach. During pregnancy, mutant mice displayed decreased luminal progenitor activity and retarded lobulo-alveolar development. Mammary glands appeared functional at the onset of lactation in mutant mice, however myoepithelial cell morphology was markedly altered, suggesting cellular compensation mechanisms involving cytoskeleton reorganization. Notably, lactation was not sustained in mutant females, and the glands underwent precocious involution. Inactivation of the p53 gene rescued the growth defects but did not restore lactogenesis in mutant mice. These results suggest that the p53 pathway is involved in the control of mammary cell proliferation and survival downstream of laminin-binding integrins and underline an essential role of cell interactions with laminin for lactogenic differentiation.



## INTRODUCTION

Mammary development begins during embryogenesis but the major steps of mammary morphogenesis and differentiation take place after birth (Macias and Hinck, 2012). At puberty, the mammary ducts grow and ramify. During pregnancy, the mammary epithelium undergoes a massive expansion characterized by ductal side-branching and the formation of alveoli, the milk-secreting units. During lactation, the gland achieves its fully differentiated phenotype, in response to the stimulus of suckling. Finally, when the offspring are weaned, the programmed death of most of the secretory epithelial cells results in post-lactational gland regression, also known as involution.

The cell fate decisions occurring during the various steps of postnatal mammary morphogenesis and differentiation are regulated mainly by systemic hormones and soluble growth factors (Brisken and Ataca, 2015). Moreover, cell interactions with the extracellular matrix (ECM) modulate cellular responses to the local signals provided by growth factors and hormones, thereby controlling all aspects of mammary gland development and function (Glukhova and Streuli, 2013; Muschler and Streuli, 2010).

The mammary epithelium comprises two layers: a layer of luminal cells, which produce milk during lactation, and a layer of basal myoepithelial cells, with contractile properties responsible for the expulsion of milk from the gland. The basal cells express the basal-specific keratins K5/K14 and smooth-muscle contractile proteins, such as  $\alpha$ -smooth muscle actin, and the transcription factors p63 and Slug. The luminal cells express K8/K18 keratins and include a population of cells expressing the receptors for estrogen and progesterone (ER and PR, respectively). These ER/PR<sup>+</sup> cells act as hormone sensors through the production of diverse paracrine signals controlling basal and luminal cell function (Brisken and Ataca, 2015).

The remarkable regenerative properties of the mammary epithelium, reflected in the replenishment of the gland in successive pregnancies, are ensured by the presence of mammary stem cells in adult tissue (Visvader and Smith, 2011). Functional studies with sorted mammary cells have revealed that the basal compartment contains multipotent stem cells from which a functional gland can be

regenerated upon transplantation, whereas the luminal cell layer contains clonogenic cells, the luminal progenitors (Asselin-Labat et al., 2007; Blaas et al., 2016; Shackleton et al., 2006; Sleeman et al., 2007; Stingl et al., 2006). This population, comprising ER/PR<sup>+</sup> and ER/PR<sup>-</sup> progenitor cells, ensures the expansion of the luminal compartment within the ducts (at puberty) and the alveoli (during pregnancy), as recently shown by lineage-tracing studies (Blaas et al., 2016; Elias et al., 2017; Rios et al., 2014; Rodilla et al., 2015; Van Keymeulen et al., 2017; Van Keymeulen et al., 2011; Wang et al., 2017). Attention has recently focused on the ER/PR<sup>-</sup> luminal progenitors, which are thought to give rise to basal-like BRCA1-associated breast tumors in humans and mice (Lim et al., 2009; Molyneux et al., 2010).

Integrins, the major cellular ECM receptors, act as membrane sensors connecting the matrix to the cytoskeleton and triggering the biochemical and mechanical signals that control cell phenotype and fate decisions (Glukhova and Streuli, 2013). Integrins are heterodimers consisting of an  $\alpha$  and a  $\beta$  subunit. Twenty-four integrin dimers with different substrate specificities have been described (Barczyk et al., 2010; Hynes, 2002). In the mammary gland, the basal cells are continuously exposed to the ECM, whereas the luminal cells form contacts with the basement membrane, particularly in the alveoli during pregnancy and lactation. Nevertheless, integrins are present in basal and luminal cells throughout the gland and at all developmental stages. Several genetic studies, including some by our group, have shown that  $\beta$ 1 integrins play an important role in controlling proliferation, survival and lactational differentiation in the mammary gland (Faraldo et al., 1998; Faraldo et al., 2002; Li et al., 2005; Naylor et al., 2005). Deletion of the  $\beta$ 1 integrin subunit gene from basal or luminal cells compromises the regenerative potential of the mammary epithelium, suggesting a role for  $\beta$ 1 integrins in the maintenance of the stem cell pool (Li et al., 2005; Taddei et al., 2008). The  $\beta$ 1 integrin chain can bind different  $\alpha$  subunits, which determine the ECM ligand specificity of the resulting dimer. Little is known about the contribution of individual integrin dimers to mammary gland development.

Like several other epithelia, the mammary bilayer sits on a specialized ECM, the basement membrane, which has laminins (LNs) as one of its major components. Pioneering studies have shown that LNs are required for the induction of lactogenic

differentiation by prolactin in cultured mammary cells (Streuli et al., 1995). Several LN-binding integrin dimers —  $\alpha 3\beta 1$ ,  $\alpha 6\beta 1$  and  $\alpha 6\beta 4$  — are present in the mammary epithelium during development (Raymond et al., 2012). Here we studied the role of these integrins in mammary development using a Cre-Lox approach in which the *Itga3* and/or *Itga6* genes were deleted *in vivo* from the luminal ER/PR<sup>-</sup> progenitor cells. We found that LN-binding integrins contributed to the regulation of luminal progenitor activity and alveologenesis during pregnancy. Moreover, in the absence of these integrins, changes in cell polarity and unscheduled involution prevented sustained lactation. Importantly, the deletion of p53 rescued the growth defects observed in the absence of LN-binding integrins, but was not sufficient for the re-establishment of correct lactogenesis, suggesting these integrins play an essential role in mammary gland differentiation.

## RESULTS

### The deletion of LN-binding integrins affects mammary alveologenesis and luminal progenitor function in pregnancy

We first assessed the expression of integrin subunits in luminal mammary cells from virgin mice by FACS analysis (Fig. S1). The two luminal populations — progenitors (mostly ER<sup>-</sup>) and mature (ER<sup>+</sup>) cells — were separated on the basis of their ICAM1 expression, as previously described (Chiche et al., 2019; Di-Cicco et al., 2015); Fig. S1A). Both luminal populations were found to express several integrin receptors on their surface, including those for laminins, collagens and fibronectin (Fig. S1B). Consistent with previous findings, luminal progenitors (ICAM1<sup>+</sup> population) expressed higher levels of  $\alpha$ 2 and  $\beta$ 3 integrins than mature luminal cells (ICAM1<sup>-</sup> population) (Asselin-Labat et al., 2007; Shehata et al., 2012). They also strongly expressed  $\alpha$ 3,  $\alpha$ 6,  $\beta$ 1 and  $\beta$ 4 integrins, the subunits of the major laminin receptors ( $\alpha$ 3 $\beta$ 1,  $\alpha$ 6 $\beta$ 1 and  $\alpha$ 6 $\beta$ 4; Fig. S1B).

To study the role of LN-binding integrins in mammary lobulo-alveolar development and lactogenic differentiation, *BlgCre* mice were crossed with mice carrying conditional alleles of the *Itga3* and *Itga6* genes (*itga3*<sup>F/F</sup> and *itga6*<sup>F/F</sup>). The *Rosa26LacZ*-reporter allele (R26R<sup>F/+</sup>) was used to monitor integrin deletion. The *Blg* promoter is active in luminal cells, from mid-pregnancy onwards (Naylor et al., 2005; Selbert et al., 1998). Consistently, immunofluorescence analysis of *BlgCre;itga3*<sup>F/F</sup>;*itga6*<sup>F/F</sup> females (referred to hereafter as  $\alpha$ 3 $\alpha$ 6KO) at 15 days of pregnancy showed a depletion of  $\alpha$ 3 and  $\alpha$ 6 integrins from most of the alveolar luminal cells (Fig. 1A). This integrin depletion in luminal cells was also confirmed by FACS and RT-qPCR analyses of mammary cells isolated from 15-day-pregnant mice (Fig. 1B, Fig. S2A,B). A previous study showed that the *Blg* promoter specifically targeted the ER/PR<sup>-</sup> luminal progenitor population (Molyneux et al., 2010). Accordingly, immunofluorescence labeling revealed that the rare cells retaining  $\alpha$ 6 integrin expression in pregnant  $\alpha$ 3 $\alpha$ 6KO mouse mammary glands also expressed PR, and therefore belonged to the ER/PR<sup>+</sup> lineage (Fig. 1C).

We then performed immunofluorescence and FACS analyses to determine whether the loss of the  $\alpha$ 3 and  $\alpha$ 6 chains affected the expression of other integrins.

Notably, surface expression of the  $\beta 1$  and  $\beta 4$  integrins was severely impaired in the luminal cells of  $\alpha 3\alpha 6$ KO females (Fig. 1A,D). The expression of other integrins was not significantly affected in luminal cells lacking LN-binding integrins (Fig. S2B,C).

Histological analysis of the mammary glands from 15-day-pregnant mice revealed an underdevelopment of the lobuloalveolar tissues in  $\alpha 3\alpha 6$ KO females, with alveolar structures that were smaller and less numerous than in control females (Fig. 1E). In agreement with the integrin expression data, X-gal staining showed that the majority of the luminal cells were LacZ<sup>+</sup>, indicating that Cre-mediated recombination had occurred in  $\alpha 3\alpha 6$ KO females (Fig. S2D). We investigated whether the observed phenotype was a consequence of impaired luminal progenitor cell activity, by performing 3D mammosphere assays with sorted luminal cells from mice at 15 days of pregnancy, as previously described (Chiche et al., 2013). Notably, the clonogenic activity of integrin-depleted luminal cells was half that in wild-type cells, whereas that of basal cells was unaffected (Fig. 1F, Fig. S2E). The mammary growth defects displayed by  $\alpha 3\alpha 6$ KO females persisted until the end of pregnancy as shown by whole mount carmine staining of mammary glands from 18-day-pregnant females and clonogenicity assays performed with sorted luminal cells (Fig. S2F,G).

Consistent with an alveolar maturation defect, RT-qPCR analyses of milk protein genes revealed significantly lower levels of *Wap*, *Lalba* and *Csn2* (encoding whey acidic protein,  $\alpha$ -lactalbumin and  $\beta$ -casein, respectively) expression in  $\alpha 3\alpha 6$ KO luminal cells from 15-day and 18-day-pregnant females (Fig. 1G, Fig. S2H). We performed mammary organoid culture, to analyze the response of the mammary epithelium to prolactin, the major regulator of lactogenic differentiation. The addition of prolactin to control explants induced the accumulation of lipid droplets in the cell cytoplasm and a 2000-fold increase in  $\beta$ -casein expression, as assessed by RT-qPCR (Fig. S3A). By contrast, cytoplasmic lipid droplets were rarely seen in  $\alpha 3\alpha 6$ KO organoids and the induction of  $\beta$ -casein in response to prolactin was severely impaired (Fig. S3A). We also used mammary organoids to analyze branching morphogenesis, which precedes alveologenesis during pregnancy. As previously described for organoids isolated from virgin females, bFGF induced growth and branching in wild-type organoids from mice at 15 days of pregnancy (Ewald et al.,

2008); Fig. S3B). By contrast,  $\alpha 3\alpha 6$ KO organoids were completely unable to branch in response to bFGF (Fig. S3B).

We performed comparative global gene expression analyses on control and  $\alpha 3\alpha 6$ KO luminal cells with Affymetrix arrays. The expression of *Muc1* and *Tjp1* (encoding the tight junction protein ZO-1), which is involved in the establishment of baso-apical polarity in the mammary epithelium, was altered in mutant cells (Fig. 1H). In addition, Reactome pathway analysis indicated lower levels of expression for circadian genes and an activation of the Rho/formins pathway in  $\alpha 3\alpha 6$ KO cells (Table S1). Other genes differentially regulated in control and mutant cells included *Lima1* and *Coro2a*, encoding proteins involved in actin regulation. Furthermore, we observed changes in the expression levels of several genes (*Mapkbp1*, *Icam1*, *Zc3h12c*) connected to the NF- $\kappa$ B signaling pathway, an important regulator of mammary alveologenesis (Fernandez-Valdivia et al., 2009). The differential expression of several genes was confirmed by RT-qPCR (Fig. 1H).

Altogether these results indicate that the depletion of LN-binding integrins affects the function of mammary luminal progenitors, perturbs mammary development and impairs lactogenic differentiation during pregnancy.

### **The deletion of LN-binding integrins affects luminal progenitor activation in response to ovarian hormones**

The ovarian hormones estrogen (E) and progesterone (P) play an important role in inducing the paracrine signals contributing to the changes occurring in the mammary gland during early pregnancy (Briskin and O'Malley, 2010). We therefore compared the responses of control and mutant epithelia to ovarian hormone treatment mimicking early events in pregnancy. The E/P stimulation of control virgin females induced intense ductal side branching accompanied by alveolus formation in the mammary glands (Fig. 2A, upper panels). By contrast, in  $\alpha 3\alpha 6$ KO glands, side branching was impaired and alveolar density was only half that in the control glands (Fig. 2A, lower panels). Consistently, proliferation was impaired in  $\alpha 3\alpha 6$ KO epithelium, as assessed by Ki67 immunolabeling (Fig. 2B). FACS analysis of E/P-stimulated glands revealed the presence of a population of luminal cells devoid of  $\alpha 6$  integrin in mutant mouse glands, confirming Blg promoter-driven Cre induction (Fig.

2C). RT-qPCR confirmed the deletion of *Itga3* and *Itga6* in  $\alpha3\alpha6$ KO luminal cells (Fig. S4A). As expected, integrin depletion occurred essentially in the ICAM1<sup>+</sup> luminal progenitor population, in which more than 70% of the cells were devoid of  $\alpha6$  integrin (Fig. 2D).

To study the individual contribution of  $\alpha3$  and  $\alpha6$  integrins in the observed phenotype, we analyzed the effect of ovarian hormone induction in *Blgcre;itga3<sup>F/F</sup>* and *Blgcre;itga6<sup>F/F</sup>* mice (referred to hereafter as  $\alpha3$ KO and  $\alpha6$ KO, respectively). The morphology of the  $\alpha3$ KO and  $\alpha6$ KO mammary glands after E/P stimulation was similar to that of the mammary glands of stimulated control littermates (Fig. S4B). Further, luminal ICAM1<sup>+</sup> progenitors were isolated from control,  $\alpha3$ KO,  $\alpha6$ KO and  $\alpha3\alpha6$ KO mammary glands as shown in Fig. S4C and their clonogenic potential was analyzed in mammosphere assays. We found that simultaneous deletion of the  $\alpha3$  and  $\alpha6$  genes, but not of either of these genes separately, significantly decreased the clonogenic capacity of luminal progenitors (Fig. 2E). In addition, expression of the milk protein genes *Wap* and *Csn2* was very weak in  $\alpha3\alpha6$ KO luminal progenitors, but not significantly affected in  $\alpha3$ KO and  $\alpha6$ KO cells (Fig. 2F). Finally, in  $\alpha3\alpha6$ KO luminal cells, the expression of *Elf5*, encoding a transcription factor essential for alveologenesis, was half that in control cells (Fig. 2F).

We previously reported that, from mid pregnancy, the luminal mammary population is particularly enriched in Sca-1-/ICAM1<sup>+</sup> cells potentially representing alveolar progenitors (Chiche et al., 2019; Di-Cicco et al., 2015). Consistently, we found that this luminal subpopulation (referred to hereafter as Lu4) was decreased in  $\alpha3\alpha6$ KO glands and displayed poor clonogenicity and low levels of milk protein gene expression (Fig. S4D-F). Notably, an efficient depletion of  $\alpha3$  and  $\alpha6$  integrins was detected in the Lu4 subpopulation, indicating that the *Blg* promoter is specifically active in these cells (Fig. S4F).

Altogether our results indicate that the  $\alpha3$  and  $\alpha6$  integrins are implicated in the response of mammary epithelial cells to ovarian hormone stimulation including luminal progenitor cell proliferation and differentiation into milk-secreting cells.

## **The deletion of LN-binding integrins leads to basal cell shape changes but does not affect early lactation**

We then analyzed the impact of LN-binding integrin gene deletion on lactation. On the second day of lactation, the mammary glands of  $\alpha3\alpha6$ KO females displayed lobuloalveolar development similar to that of the control glands, with dense secretory tissue and almost no fat pad stroma (Fig. 3A). Levels of milk protein gene transcripts in the luminal cells of  $\alpha3\alpha6$ KO mice were not significantly different from those in control mice, indicating that the alveoli were functional (Fig. 3B). Consistently, the weights of pups fed by control and mutant females were similar on day 2 of lactation (Fig. 3C). However, the level of phosphorylation of FAK, an important downstream effector of integrins, was lower in  $\alpha3\alpha6$ KO glands (Fig. S5A).

The depletion of LN-binding integrins was confirmed by FACS or RT-qPCR (Fig. S5B,C). Morphological analyses of the mammary glands in early lactation were performed by the double immunofluorescence labeling of tissue sections. Consistent with FACS analysis, the luminal cells of mutant glands were devoid of  $\alpha6$  integrin, whereas this integrin was detected in the basal cells (Fig. 3D, Fig. S5B). In sections through control glands, basal myoepithelial cells, detected by  $\alpha$ -smooth muscle ( $\alpha$ SMA) labeling, appeared as rare spots decorating the basal side of the alveoli. By contrast, the myoepithelial cells in integrin-depleted glands formed a more continuous layer around luminal cells (Fig. 3D, upper panels). Confocal microscopy revealed that myoepithelial cell shape was profoundly altered in the mammary alveoli of  $\alpha3\alpha6$ KO females (Fig. 3D, lower panels). In particular, the myoepithelial cells in the mutant epithelium had thicker protrusions and covered a larger area of the alveoli than the myoepithelial cells of control glands (Fig. 3D-F). To investigate the molecular alterations accounting for these morphological changes we performed RNAseq analysis on freshly sorted basal cells from control and  $\alpha3\alpha6$ KO mice. Several genes (including *Nectin2*, *Gjc1*, *Cldn15*, *Emb* and *Lama5*), encoding proteins involved in cell-cell or cell-substrate adhesion were more strongly expressed in mutant females than in controls (Fig. 3G). In addition, we observed changes in the expression of numerous genes involved in the regulation of actin dynamics and cell shape (Fig. 3G).



These results reveal that, at the beginning of lactation, the mammary alveoli of mutant females, present major alterations in basal cell morphology, despite being apparently functional.

### **LN-binding integrin depletion disturbs luminal cell baso-apical polarization and leads to unscheduled involution**

We investigated whether lactation could proceed normally beyond day 2 in the absence of LN-binding integrins, by comparing the mammary phenotypes of control and mutant females at the time of pup weaning on day 21. The glands from  $\alpha3\alpha6$ KO females presented collapsed, dispersed alveolar structures reminiscent of those found in involuting tissues, a morphology different from that of control tissue (Fig. 4A, Fig. S6A). The glands of  $\alpha3$ KO females were similar to those of control animals, whereas  $\alpha6$ KO females displayed slightly less developed glands (Fig. 4A). Pups fed by  $\alpha3\alpha6$ KO females were significantly lighter than pups fed by control mice, from day 14 of lactation (Fig. 4B). Consistently, the level of expression of milk protein genes was significantly lower in  $\alpha3\alpha6$ KO glands (Fig. 4C). The pups fed by  $\alpha3$ KO females were of normal weight, whereas those fed by  $\alpha6$ KO females were significantly lighter, after 21 days of lactation (Fig. 4B). At this stage, the expression of milk protein genes was impaired in  $\alpha6$ KO glands (Fig. S6B).

A more detailed histological analysis of glands at 14 days of lactation revealed that, unlike the flat luminal cells typically observed in control alveoli full of milk, the luminal cells in  $\alpha3\alpha6$ KO tissue were frequently protruding into the lumen (Fig. 4D, Fig. S6C). Using immunofluorescence labeling we analyzed the distribution of polarity markers in  $\alpha3\alpha6$ KO epithelium. The *cis*-Golgi marker protein GM130, which was located in an apical position facing the lumen in control luminal cells, was abnormally distributed in about 12% of luminal cells of  $\alpha3\alpha6$ KO alveoli (Fig. 4E,F). Two types of abnormal Golgi localization were observed: cells in which GM130 labeling revealed a normal ribbon-like Golgi with aberrant basal localization (Fig. 4E, central picture) and cells with a dispersed Golgi, also basally located with respect to the nucleus (Fig. 4E, right picture). In these abnormal mutant cells, the polarity marker Par3, normally presenting an apico-lateral distribution in control epithelium, was either absent or basally located, indicating a disruption of polarity (Fig. 4F). In addition, E-cadherin was often found at the apical side of luminal  $\alpha3\alpha6$ KO cells with

aberrant morphology (Fig. 4G). Although immunolabelling for Laminin did not reveal major perturbations in basement membrane integrity (Fig. 4G), expression of *Lamb3*, a gene coding for  $\beta 3$  chain, a component of Laminin 332 (Laminin-5), one of the major constituents of the mammary basement membrane, was increased in  $\alpha 3\alpha 6$ KO glands (Fig. S6D). Finally, FAK phosphorylation levels were lower in  $\alpha 3\alpha 6$ KO glands at lactation day 14, confirming a perturbation of luminal cell interactions with ECM (Fig. S6E).

The secretory tissue hypoplasia observed in  $\alpha 3\alpha 6$ KO glands suggested that precocious cell death might be associated with LN-binding integrin deletion. To analyze apoptosis rates in mammary tissues lacking LN-binding integrins, we performed TUNEL assays with sections through day 21 lactating glands; the number of TUNEL-positive cells was greater in  $\alpha 3\alpha 6$ KO females (Fig. 4H). Increases in cathepsin D expression and lysosomal release during involution-associated cell death have recently been reported (Sargeant et al., 2014). Consistently, cells expressing cathepsin D were detected in the mutant tissue (Fig. S6F). Finally, the expression of *Lif* (encoding leukemia inhibitory factor), an essential factor for the regulation of cell death during mammary involution, was strongly increased during late lactation in  $\alpha 3\alpha 6$ KO tissues (Kritikou et al., 2003; Schere-Levy et al., 2003); Fig. 4I).

Together, these results show that the depletion of LN-binding integrins in luminal cells perturbs baso-apical polarization and induces early cell death and unscheduled secretory tissue involution, preventing full lactation.

### **Genetic p53 suppression restores growth but not differentiation in mammary luminal cells depleted of LN-binding integrins**

We recently showed that, in the absence of LN-binding integrins, the clonogenic activity of basal mammary cells was inhibited by a mechanism involving p53 activation (Romagnoli et al., 2019). Analysis of the microarray data obtained with 15-day pregnant mouse glands suggested an activation of the p53 pathway in  $\alpha 3\alpha 6$ KO luminal cells (Fig. 5A). Consistently, in the mammospheres generated by these cells, the expression of *Cdkn1a* (coding for the cell cycle inhibitor p21) and *Mdm2*, two important p53 targets, was increased, as assessed by qPCR analysis

(Fig. 5B). To study the possible involvement of p53 deregulation in the abnormal mammary phenotype of  $\alpha3\alpha6$ KO mice, we crossed these mice with mice carrying conditional alleles of the *Trp53* gene (*Trp53<sup>Flox</sup>*) to obtain *Blgcre;itga3<sup>F/F</sup>;itga6<sup>F/F</sup>;Trp53<sup>F/F</sup>* mice (referred to hereafter as  $\alpha3\alpha6p53$ KO). Following stimulation with ovarian hormones, the mammary glands of  $\alpha3\alpha6p53$ KO females presented normal side branching and an alveolar density similar to that found in control littermates (Fig. 5C). The mammospheres formed by  $\alpha3\alpha6p53$ KO cells did not express  $\alpha6$  integrin, confirming target gene deletion (Fig. 5D). Quantitative analysis revealed that the clonogenic activity of  $\alpha3\alpha6p53$ KO luminal progenitors was unaffected and similar to that in the controls in 1<sup>st</sup>- and 2<sup>nd</sup>-generation mammosphere assays (Fig. 5D, Fig. S7A). Nevertheless, milk protein gene expression levels were significantly lower in the  $\alpha3\alpha6p53$ KO luminal progenitors, indicating differentiation defects (Fig. 5E). Consistently, in mammary organoids derived from 15-day-pregnant  $\alpha3\alpha6p53$ KO glands, the expression of *Csn2* after prolactin induction was decreased when compared to control organoids (Fig. S7B). When treated with bFGF,  $\alpha3\alpha6p53$ KO organoids displayed active growth, but failed branching (Fig. S7C).

We further analyzed  $\alpha3\alpha6p53$ KO mammary glands during lactation and found that, on day 14, alveolar morphology was altered with respect to control glands, with  $\alpha3\alpha6p53$ KO alveoli resembling those found in  $\alpha3\alpha6$ KO tissue (Fig. 5F). As in p53-expressing epithelium, myoepithelial cell morphology appeared altered in the  $\alpha3\alpha6p53$ KO lactating glands as shown by the increased alveolar surface covered by basal cells (Fig. S7D). Interestingly, proliferating cells, rarely found in control or  $\alpha3\alpha6$ KO glands at 14 days of lactation, were readily detected in  $\alpha3\alpha6p53$ KO epithelium (Fig. S7D). In addition, as in  $\alpha3\alpha6$ KO p53-proficient mice, the GM130 Golgi marker, Par3 and E-cadherin were frequently mislocalized, indicating alterations in epithelial cell polarity (Fig. 5G, Fig. S7E,F). The number of TUNEL-positive cells and the level of expression of *Lif* in  $\alpha3\alpha6p53$ KO glands on day 21 of lactation were similar to those in controls, indicating that p53 deletion interfered with the cell death caused by integrin deletion (Fig. S7G,H). However, the pups fed by  $\alpha3\alpha6p53$ KO mice were lighter than those fed by control mice from the middle of

lactation onwards, and, consistently, the levels of expression of milk protein genes were significantly reduced (Fig. 5H,I).

These results indicate that genetic inactivation of p53 rescues the growth defects, but not the impairment of epithelial polarity and lactogenic differentiation caused by the depletion of LN-binding integrins.

### **Activation of a Rho/MyosinII/p53 pathway following depletion of LN-binding integrins in mammary luminal progenitors**

We have recently reported that LN-binding integrins play an essential role in controlling the proliferative potential of mammary basal stem/progenitor cells through RhoA/ROCK/MyosinII-mediated regulation of p53 (Romagnoli et al., 2019). To study if a similar pathway operates in luminal progenitor cells, we isolated luminal ICAM<sup>+</sup> cells from control,  $\alpha3\alpha6$ KO and  $\alpha3\alpha6$ p53KO virgin females and deleted the *Itga3*, *Itga6* and *Trp53* genes *in vitro* by transduction with an adenovirus expressing Cre-recombinase (Adeno-Cre). Gene deletion was confirmed by RT-qPCR analyses (Fig. S8A). Consistent with the results obtained with freshly isolated luminal progenitors from pregnant mice, the clonogenicity of luminal progenitors was severely impaired after depletion of LN-binding integrins *in vitro* (Fig. 6A). RT-qPCR analyses performed with RNA samples obtained from dissociated mammospheres revealed an upregulation of p53 transcriptional targets such as *Cdkn1a* and *Mdm2* in  $\alpha3\alpha6$ KO cells, suggesting an activation of the p53 pathway in these cells (Fig. 6B, Fig. S8B). Furthermore, depletion of p53 rescued the mammosphere formation capacity of  $\alpha3\alpha6$ KO luminal progenitors (Fig. 6A).

Western blot analysis showed that phospho-MLC levels were increased in  $\alpha3\alpha6$ KO cells indicating enhanced RhoA/ROCK activity (Fig. S8C). Consistently, analysis of the microarray data obtained from 15-day pregnant glands suggested an enhanced Rho activity in  $\alpha3\alpha6$ KO luminal cells compared to control cells (Fig. S8D). Next, to study whether activation of the RhoA/ROCK/Myosin II pathway could account for the impaired  $\alpha3\alpha6$ KO luminal progenitor activity, we performed mammosphere assays in the presence of the ROCK inhibitor Y27632 or Blebbistatin, an inhibitor of Myosin II activity downstream from ROCK. As shown in Fig. 6C, in the presence of Y27632 or Blebbistatin, the clonogenic capacity of  $\alpha3\alpha6$ KO cells was

restored, whereas control cells presented an increase in sphere formation capacity (Fig. 6C). In contrast, these inhibitors had little effect on the clonogenicity of  $\alpha3\alpha6p53KO$  cells (Fig. 6C).

We next studied the effects of Y27632 and Blebbistatin on p53 activity in control and integrin-depleted cells. Expression of the p53 target genes *Cdkn1a* and *Mdm2* was downregulated in the presence of the drugs, in control and mutant cells, suggesting an inhibition of p53 transcriptional activity (Fig. 6D, Fig. S8B). In line with these data, p53 protein was nearly undetectable in control cells treated with Y27632 or Blebbistatin (Fig. 6E). Further, the p53 protein levels were increased in  $\alpha3\alpha6KO$  cells. Consistently, this was accompanied by a decreased level of MDM2, a protein facilitating the p53 proteosomal degradation (Carr and Jones, 2016; Fig. 6E). Finally, inhibition of Myosin II by Y27632 or Blebbistatin resulted in an increase in MDM2 protein and a decrease in p53 levels in  $\alpha3\alpha6KO$  cells (Fig. 6E).

Taken together, these data strongly indicate that the p53 pathway activation in the luminal progenitors lacking LN-binding integrins, is mediated by Rho/ROCK/MyosinII axis.

## DISCUSSION

This study implicates LN-binding integrins containing  $\alpha 3$  or  $\alpha 6$  subunits in the control of luminal progenitor expansion and alveologenesis during pregnancy and demonstrates the requirement of these integrins for the maintenance of functional secretory tissue in lactation.

Mammary basal cells are highly enriched in integrins, but luminal cells also express a panel of different integrins on their surface (Glukhova and Streuli, 2013; Raymond et al., 2012). In adult virgin mice, integrin dimers including  $\alpha 2$  or  $\beta 3$  subunits, mostly functioning as receptors for collagen and fibronectin, respectively, have been used as markers for separating the luminal progenitor population from the population of ER/PR<sup>+</sup> luminal cells (Asselin-Labat et al., 2007; Shehata et al., 2012). However, the role of specific integrin dimers in luminal progenitor function during mammary development has yet to be analyzed in detail.

Here, to study the roles played by LN-binding integrins in mammary luminal cells, we specifically targeted Cre expression to the luminal progenitor population with the BLG promoter, permitting deletion of  $\alpha 3$  and/or  $\alpha 6$  integrin chains from luminal progenitors. We found that the depletion of LN-binding integrins interfered with the expansion of luminal progenitors in pregnancy or following E/P administration. Branching morphogenesis and alveologenesis were subsequently impaired, leading to differentiation defects in the mammary epithelium of pregnant or E/P-treated mutant mice. Deletion of the p53 gene rescued hormone-induced alveolar development in  $\alpha 3\alpha 6$ KO mice, suggesting that, as previously reported for basal cells, p53 activation may contribute to the mammary growth defects observed in luminal cells depleted of LN-binding integrins (Romagnoli et al., 2019). Deletion of the gene encoding p21, which is involved in cell cycle control downstream from p53, has been shown to rescue the proliferation defects observed in cultured mammary epithelial cells lacking  $\beta 1$  integrin (Li et al., 2005). Consistently with the data obtained *in vivo*, we found that: 1) clonogenicity of luminal progenitors was severely impaired after adenoCre-mediated depletion of LN-binding integrins *in vitro*; 2) p53 pathway was activated in these cells, and depletion of p53 rescued the mammosphere formation capacity of  $\alpha 3\alpha 6$ KO luminal progenitors, and 3) as previously found in

basal cells (Romagnoli et al., 2019) a Rho/ROCK/MyosinII axis contributed to the activation of p53 pathway in the luminal progenitors depleted of LN-binding integrins.

Importantly, despite the restoration of hormone-induced alveologenesis by p53 inactivation in  $\alpha3\alpha6$ KO mice, milk protein transcript levels remained low, indicating that, as suggested by pioneering *in vitro* studies from Bissell's group, LN-binding integrins are essential for lactogenic differentiation (Muschler et al., 1999).

Surprisingly, at the onset of lactation, mammary glands in which the luminal cells lacked LN-binding integrins appeared to be well-developed and functional. The altered morphology of the alveolar myoepithelial cells observed in mutant mice might provide an explanation for this. Indeed, the alveolar myoepithelial cells from  $\alpha3\alpha6$ KO mice were more spread out at the onset of lactation than control basal cells, limiting the contact of  $\alpha3\alpha6$ -integrin-depleted luminal cells with the basement membrane. RNAseq analysis showed that myoepithelial cells from  $\alpha3\alpha6$ KO mice displayed changes in the expression of genes involved in the regulation of cell adhesion and actin dynamics that might account for the observed alteration of cell shape. These findings suggest that cellular compensation mechanisms involving basal myoepithelial cells may contribute to the maintenance of alveolar architecture in  $\alpha3\alpha6$ KO mice. One possible explanation for the changes in myoepithelial cell phenotype would be a strengthening of their interactions with luminal cells depleted of LN-binding integrins since cell-cell and cell-ECM adhesions have been reported to exert negative feedback on each other (Burute and Thery, 2012). Another hypothetical mechanism could involve the tension forces exerted by the stroma on alveolar cells and mechano-transduction via cell-ECM adhesions including integrins (Glukhova and Streuli, 2013). Indeed, in normal alveoli, stroma exerts tension on both, luminal and myoepithelial cells, whilst in  $\alpha3\alpha6$ KO glands, luminal cells lacking LN-binding integrins, forces might be redistributed on the myoepithelial cells inducing their cytoskeleton changes.

We found that  $\alpha3\alpha6$ KO mice were unable to sustain lactation up to day 21, and by day 14, the pups fed by these mutant mice were already significantly lighter than those fed by control mice. By day 21, the glands from mutant females presented signs of premature involution, with collapsed alveoli and detached secretory cells in the lumen.

The interaction of integrin receptors with LN is known to be essential for the establishment of epithelial cell baso-apical polarity (reviewed in Lee and Streuli, 2014). Consistently, in  $\alpha3\alpha6$ KO females, by day 14 of lactation, numerous luminal cells had an aberrant morphology. These cells were not flattened like those in control tissues, and displayed signs of a disruption of baso-apical polarity, with mislocalized Par3 and E-cadherin and dispersed or basally localized Golgi. These data suggest that milk secretion was impaired in  $\alpha3\alpha6$ KO females at peak lactation, as the formation and secretion of milk vesicles requires normal Golgi function and luminal cell polarization (Truchet and Honvo-Houeto, 2017). Importantly, in  $\alpha3\alpha6p53$ KO 14-day-lactating glands, morphological and polarity defects were also detected in luminal cells concomitantly with perturbed lactogenic gland differentiation.

In their seminal work, Streuli's team reported that the basement membrane was essential for the survival of mammary epithelial cells (Pullan et al., 1996). Consistent with this finding, we previously showed that the expression of a dominant-negative  $\beta1$ -integrin mutant induced apoptosis early in lactation (Faraldo et al., 1998). In  $\alpha3\alpha6$ KO mice, morphological alterations were visible in alveolar luminal cells at 14 days of lactation, but increases in apoptosis and lysosome/cathepsin-associated cell death were not detected in the mutant glands until day 21 of lactation, when the mutant glands began to undergo unscheduled involution. Notably, the apoptosis observed in late lactation in  $\alpha3\alpha6$ KO females was completely abolished by p53 gene deletion, consistent with the proposed role for p53 in the triggering of cell death during the first few days of mammary involution (Jerry et al., 2002; Jerry et al., 1998). The occurrence of cathepsin-associated cell death, reported by Watson's team to be the major cell death mechanism induced by milk stasis during post-lactation involution, is consistent with an impairment of milk secretion in mutant glands (Sargeant et al., 2014).

Klinowska et al. have reported that lobulo-alveolar development could occur in the absence of  $\alpha3$  or  $\alpha6$  chain-containing integrins although that study did not present any quantitative evaluation of lactogenic differentiation in mutant epithelium (Klinowska et al., 2001). Consistently, we found that mammary glands depleted in luminal cells of  $\alpha3$  integrin appeared normal whereas  $\alpha6$  depletion led to mild gland hypoplasia with a minor, but measurable decrease in lactational differentiation. Only



the simultaneous depletion of both the  $\alpha 3$  and  $\alpha 6$  integrins led to a significant perturbation of mammary development and function. The difference in phenotypes following the deletion of  $\alpha 3$  or  $\alpha 6$  alone is consistent with the non-redundant cellular functions of these integrins. Indeed, unlike  $\alpha 3$ ,  $\alpha 6$  can associate with  $\beta 4$  and the  $\alpha 6\beta 4$  dimer, unlike  $\beta 1$ -containing integrins, is a component of hemidesmosomes. A recent study reported that deletion of  $\beta 4$  integrin from luminal cells induced defects in alveologenesis and milk production during pregnancy (Walker et al., 2020). Thus, the decreased  $\beta 4$ -integrin surface levels detected in  $\alpha 3\alpha 6$ KO luminal cells could contribute to the observed phenotype.

We previously showed that  $\alpha 3$  integrin is essential for the contractile function of basal myoepithelial cells during lactation (Raymond et al., 2011). These previously described mutant mice depleted of  $\alpha 3\beta 1$  integrin in the basal mammary epithelial layer, displayed milk stasis, and their glands were engorged with milk. Importantly, in  $\alpha 3\alpha 6$ KO animals presenting integrin deletion in luminal compartment only, milk stasis was not observed strongly indicating that apparently, the contractile activity was not perturbed in the myoepithelial cells of  $\alpha 3\alpha 6$ KO mice.

Previous studies have shown that the depletion of  $\beta 1$  integrins or the disruption of their function by the expression of a dominant-negative mutant in mammary luminal cells affects gland growth and differentiation (Faraldo et al., 1998; Li et al., 2005; Naylor et al., 2005). The mammary phenotype observed in mice in which the luminal cells were depleted of  $\beta 1$ -integrins was more severe than the one observed here, with the mutant mice frequently unable to feed normal-size litters and, in the most extreme cases, total lactation failure. The  $\beta 1$  integrin subunit forms dimers with several different  $\alpha$  subunits. Its depletion would therefore be expected to affect receptors not only for LN, but also for other ECM proteins, such as fibronectin, which has been shown to be essential for lobuloalveolar differentiation during pregnancy (Liu et al., 2010).

In recent decades, numerous studies have provided evidence for a role of LN-binding integrins in tumorigenesis, and both tumor-suppressing and tumor-promoting activities have been reported, depending on the cellular context (Ramovs et al., 2017). Importantly, luminal progenitors, the cell population targeted for integrin depletion in our model, are thought to be at the origin of basal-like breast tumors (Lim

et al., 2009; Molyneux et al., 2010). In light of our data, it would be of interest to investigate the contribution of LN-binding integrins to basal-like breast cancer induction and progression, and, in particular, the contribution of these molecules to the regulation of cancer stem cells, which are often responsible for tumor relapse and therefore, suitable therapeutic cell targets in this poor prognosis disease.

## **MATERIAL AND METHODS**

### ***Mice***

The generation of *Itga3*<sup>F/F</sup>, *Itga6*<sup>F/F</sup> and *Trp53*<sup>F/F</sup> mice has been previously described (De Arcangelis et al., 2017; Jonkers et al., 2001; Margadant et al., 2009). *BlgCre* transgenic mice were purchased from The Jackson Laboratory and *Rosa26LacZ* reporter strain was kindly provided by Dr. Soriano (Soriano, 1999). Mice were bred in a mixed CBA/C57Bl6 background. In all experiments *BlgCre*-negative littermates were used as controls. For pup weigh measure, the litters of 8 pups were analyzed. The care and use of animals were conducted in accordance with the European and National Regulations for the Protection of Vertebrate Animals used for Experimental and other Scientific Purposes (facility license C750517/18). All experimental procedures were ethically approved (ethical approval 02265.02).

### ***Whole-mount analyses, histology and immunolabeling***

For whole-mount Carmine-Alum staining, dissected mammary fat pads were spread onto glass slides, fixed in a 1/3/6 mixture of acetic acid/chloroform/methanol and stained as described elsewhere (Teuliere et al., 2005). For whole-mount X-gal staining, mammary glands were fixed in 2.5% paraformaldehyde in PBS, pH 7.5, for 1 hour at 4°C, and stained overnight at 30°C (Biology of the Mammary Gland, <http://mammary.nih.gov>). For histological analyses, glands were embedded in paraffin, and seven µm-thick sections were cut and de-waxed for Fast Red counterstaining (X-gal-stained whole-mount glands), haematoxylin/eosin staining or immunolabeling. For alveolar density estimation the whole surface occupied by alveoli was reported to the total mammary tissue surface using ImageJ on micrographs of H/E stained sections. For cryosections, glands were frozen on Tissu-Tek (Sakura) and thin (5 µm) or thick (30 µm) sections were obtained using a Leica Cryostat. Thick sections were used to calculate basal cell parameters in lactating glands using Image J. Basal cells were immunolabeled with anti- $\alpha$ -smooth muscle actin antibody and their surface was measured in at least 30 alveoli from 3 mice per genotype. Branch width of basal cells was measured at the proximal part of the branch. A total of at least 100 branches in 3 mice per genotype were evaluated. The following primary antibodies were used for immunolabeling: mouse monoclonal anti- $\alpha$ -smooth muscle actin (Sigma-Aldrich A2547, 1/200), anti-Keratin 8 (Covance MMS-

162P, 1/100) and anti-GM130 (BD Biosciences 610823, 1/100); rat monoclonal anti- $\beta$ 4 integrin (BD Biosciences clone 346-11A, 1/100) anti- $\alpha$ 6 integrin (Biolegend clone GoH3, 1/200) anti- $\beta$ 1 integrin (Millipore MAB1997, 1/100) and anti-E-cadherin (Life Technologies, 1/250); rabbit polyclonal anti  $\alpha$ 3 integrin (#141742;(Sachs et al., 2006), anti-PR (Santa Cruz Biotechnology 7208, 1/200), anti-pankeratin (Dako Z0622, 1/100), anti-Par3 (Millipore, 07-330, 1/100), anti-Ki67 (Labvision/Neomarkers, 1/200) and anti-laminin 5 (a kind gift of M. Aumalley, University of Cologne, Germany); goat polyclonal anti-cathepsin D (Sicgen AB0043, 1/100). Alexafluor-conjugated secondary antibodies (Molecular Probes) were used at 1/500 dilution. Image acquisition was performed using a Leica DM 6000B microscope or a Nikon confocal A1r microscope.

### ***TUNEL analysis***

For cell death analysis, glands were fixed in 4% paraformaldehyde in PBS, pH 7.5, O/N at 4°C. Seven  $\mu$ m paraffin sections were analyzed for TdT digoxigenin nick-end labeling with Apoptag Plus (Sigma Aldrich) following manufacturer's instructions. After counterstaining with methyl green, 1500-2000 cells nuclei/sample were counted.

### ***Mammary gland dissociation, cell sorting and flow cytometry analysis***

Thoracic and inguinal mammary glands were pooled, dissociated and processed for single-cell suspension and flow cytometry as described elsewhere (Di-Cicco et al., 2015; Stingl et al., 2006; Taddei et al., 2008). For cell sorting, cells were incubated at 4°C for 20 min with the following antibodies: anti-CD45-APC (clone 30-F11), anti-CD31-APC (clone MEC13.3), anti-CD24-BViolet421 (clone M1/69), and anti-CD49f-PeCy7 (clone GoH3), or anti-ICAM1-PeCy7 (clone YN1/1.7.4), anti-Sca-1-PE (clone E13-161.7), all from Biolegend. Labelled cells were analyzed and sorted out using a MoFlo Astrios cell sorter (Beckman Coulter). Sorted luminal progenitor cells (CD31/45<sup>-</sup>, CD24<sup>high</sup> CD49f<sup>low</sup> ICAM<sup>+</sup> population) were used for mammosphere assays and gene expression analysis. Sorted cell population purity was at least 95%. The antibodies used for the analysis of cell surface integrin expression in basal and luminal cells are presented in Table S2. Data were analyzed using FlowJo software.

### ***Estrogen/progesterone stimulation experiments***

For hormone stimulation, estrogen/progesterone silicon implants (E/P) from Belma Technologies were subcutaneously implanted into 12-weeks virgin females as previously described (Rajkumar et al., 2007). After 30 days, mammary glands #1 and 2 were collected for whole-mount Carmine staining and histological analyses, while glands #3, 4 and 5 were pooled for dissociation and cell sorting as described below.

### ***Organoids and mammospheres cell culture***

Mammary organoids obtained as previously described (Ewald et al., 2008) were resuspended in Growth Factor Reduced Matrigel (BD Biosciences) and grown in 8-well coverslip bottom chambers (Ibidi). A suspension containing 300 organoids in 30  $\mu$ l of Matrigel was added to each well. After 30 min at 37°C, minimal media was added: DMEM/F12, 1% v/v insulin, transferrin, selenium (Sigma Aldrich) and 1% penicillin/streptomycin. When indicated, prolactin (R&D systems, 40nM) or bFGF (GIBCO, 5 nM) was added to the medium after 1-2 hours of culture and the medium was renewed every 2 days. Organoids were imaged using a Nikon Ni-E microscope, immunolabelled and visualized in a Nikon confocal A1r microscope or collected and analyzed for gene expression as indicated above.

For mammosphere cultures, freshly isolated luminal cells were seeded on ultralow-adherence 24-well plates (Corning) at the density of 10000 cells/well, in mammosphere media: DMEM/F12 medium supplemented with B27 diluted 1/50 (GIBCO), 20ng/mL EGF, (Invitrogen), 20 ng/mL bFGF (GIBCO), 4  $\mu$ g/mL heparin (Sigma-Aldrich), 10  $\mu$ g/mL insulin (Sigma-Aldrich) and 2% Matrigel (BD Pharmingen) as described (Chiche et al., 2013). After 12-14 days of culture, wells were photographed and mammospheres counted using ImageJ software then collected for RNA extraction and gene expression analysis.

### ***Adeno-Cre mediated gene deletion***

Freshly sorted luminal progenitor cells (CD31/45<sup>-</sup>, CD24<sup>high</sup> CD49f<sup>low</sup> ICAM<sup>+</sup> population) were incubated with an adenovirus expressing the Cre recombinase under the control of the CMV promoter (AdCre, SignaGen Laboratories) at MOI of 4000 for 1 hour at 37°C. After washing, cells were resuspended in mammosphere medium at the density of 7000 cells/well. For ROCK or Myosin II-ATP-ase inhibition, Y27632 (1  $\mu$ M, Millipore) or Blebbistatin (5  $\mu$ M, R&D Systems) were added to the

mammosphere medium and replenished twice a week. After 12 days of culture, wells were photographed and the number of mammospheres was analyzed using ImageJ software.

### **Western blot analysis**

Mammary tissue samples were homogenized in RIPA extraction buffer (40 mM Tris pH 7.5, 276 mM NaCl, 2% Nonidet P-40, 4 mM EDTA) in the presence of protease and phosphatase inhibitors (ThermoScientific) following further incubation during 20 min at 4°C in a rotation wheel. BCA Protein Assay (Pierce) was used to estimate protein concentration. 50 µg of protein extracts were boiled for 5 min in Laemli buffer before migration. Mammosphere pellets were resuspended in 1;5x hot Laemli buffer, vortexed and boiled for 5 min. Samples were run on NuPAGE Novex 4-12% Bis Tris gels (Life Technologies/Invitrogen) and transferred onto nitrocellulose. Membranes were incubated with 5% BSA in TBS containing 0.1% Tween 20 (TBST) for 1 hour at room temperature and with primary antibodies overnight at 4°C. The following primary antibodies were used: anti-p53 (clone 1C12, Cell Signalling Tech), anti-MDM2 (clone EP16627; Abcam), anti-P-FAK-Tyr397 (Cell Signalling Tech.), anti-FAK (Transd. Laboratories), anti-P-MLC-Ser19, anti-MLC (Cell Signalling Tech.), and anti-GAPDH (clone FL-335, Santa Cruz Biotech.) Secondary antibodies coupled to horseradish peroxidase were from Cell Signalling Tech. Detection was performed by chemiluminescence (Super signal West Pico+, Pierce). Quantitative analysis was performed with ImageJ.

### **RNA extraction and RT-qPCR**

RNA was isolated from whole mammary glands using Trizol reagent (Life Technologies) and further purified on a cleanup column (Qiagen). For mammosphere and organoid RNA extraction, RNeasy Microkit was used. To avoid eventual DNA contamination, purified RNA was treated with DNase (Qiagen). RNAs were reverse-transcribed using MMLV H(-) Point reverse transcriptase (Promega). Quantitative PCR was performed using the QuantiNova SYBR Green PCR Kit (Qiagen) on a LightCycler 480 real-time PCR system (Roche). The values obtained were normalized to *Gapdh* levels. The primers used for RT-qPCR analysis were purchased from SABiosciences/Qiagen or designed using Oligo 6.8 software (Molecular biology Insights) and synthesized by Eurogentec. Primers used in this study are listed in Table S3.

### ***Microarray analysis***

Global gene expression analysis was performed with total RNA extracted from sorted luminal cells. RNA quality control was performed with an Agilent 2100 Bioanalyzer (Agilent Technologies, Santa Clara, CA, USA). The WT-Ovation™ Pico RNA Amplification system (Nugen) was applied from 1 ng of total RNA to generate sufficient amount of biotinylated cDNA. Samples were hybridized on Affymetrix GeneChip Mouse Genome ClariomS arrays. Analyses were made using EASANA® (GenoSplice, [www.genosplice.com](http://www.genosplice.com)), which is based on the GenoSplice's FAST DB® release 2014\_2 annotations (de la Grange et al., 2005). Data were normalized using quantile normalization and an unpaired Student's t-test was used to compare gene intensities in the different samples. Genes were considered significantly regulated when fold-change between the compared groups was  $\geq 1.5$  and uncorrected P-value  $\leq 0.05$ . The molecular and functional interactions of the genes identified were analyzed with REACTOME pathway analysis. The microarray data are available in GEO (accession number: GSE132349).

### ***RNA sequencing***

cDNA was generated from total RNA by the SMART-seq V4 Ultra-low input kit, subjected to quality control on a BioAnalyzer and accurately quantified using a Qubit fluorometer. Libraries were prepared from 0.6ng of cDNA using the Illumina Nextera XT library preparation kit according to the manufacturer instruction. Sequencing was carried out using 2\*100 cycles (paired-end reads, 100 nucleotides) on an Illumina HiSeq2500 instrument (rapid flow cells) to get around 20M paired reads per sample. Quality assessment on data confirmed good complexity of libraries and low duplicate rate (less than 10%). RNA-Seq data analysis was performed by GenoSplice technology ([www.genosplice.com](http://www.genosplice.com)). Sequencing, data quality, reads repartition and insert size estimation were performed using FastQC, Picard-Tools, Samtools and rseqc. Reads were mapped using STARv2.4.0 on the mm10 Mouse genome assembly (Dobin et al., 2013). Normalization and differential gene expression were performed using DESeq2 (Love et al., 2014) on R (v.3.1.3). Genes were considered as expressed if their rpkms value was greater than 97.5% of the background rpkms value based on intergenic regions. Results were considered statistically significant for unadjusted p-values  $\leq 0.05$  and fold-changes  $\geq 1.5$ . The RNAseq data are available in GEO (accession number: GSE132281).

### **Statistical analysis**

All values are shown as mean  $\pm$  standard deviation (SD). P values were determined using Student's t test with two-tailed distribution and unequal variance (Welch's correction). All statistical analyses were performed using GraphPad Prism v6 software.

### **ACKNOWLEDGEMENTS**

We are particularly grateful to C. Lambert for technical assistance, to Dr. I. Grandjean, S. Jannet and the personnel of the animal facilities at Institut Curie for taking care of the mice, to Z. Maciorowski, A. Viguiet and S. Grondin for excellent assistance with FACS analyses and to the Cell and Tissue Imaging (PICT-IBiSA), Institut Curie, member of the French National Research Infrastructure France-BioImaging (ANR10-INBS-04). We also thank Drs. K. Raymond and S. Cagnet for obtaining mice, Drs. P. Soriano and J. Jonkers for providing mouse strains and Dr. K. Raymond for helpful discussion.

### **COMPETING INTERESTS**

The authors declare no competing or financial interests.

### **AUTHOR CONTRIBUTIONS**

Conceptualization: M.R., M.A.G., M.M.F; Methodology: M.R., L.B., S.B., P.G., M.A.D. M.A.G., M.M.F; Investigation: M.R., L.B., M.P.L., A.D.C., S.B., P.G., M.A.D., M.M.F; Resources: A.A., E.G.L., A.S.; Writing: M.R., M.A.G., M.M.F; Funding acquisition: M.R., M.A.D., M.A.G., M.M.F.

### **FUNDING**

The work was supported by grants from *Agence Nationale de la Recherche* (ANR-13-BSV2-0001), 2014-1-SEIN-01-ICR-1 grant from *l'Institut National de Cancer, la Fondation ARC* and *La Ligue Contre le Cancer Ile de France (Comité de Paris, RS16/75-70 and RS19/75-67; Comité de l'Essonne M27216)* and Labex Celtisphybio (ANR-10-LABX-0038), part of the Idex PSL. MR received funding from Marie Curie Fellowship Program. High-throughput sequencing has been performed by the ICGex NGS platform of the Institut Curie supported by the grants ANR-10-EQPX-03, ANR-10-INBS-09-0 and Canceropole Ile-de-France (INCa-DGOS-4654).



## REFERENCES

- Asselin-Labat, M.L., Sutherland, K.D., Barker, H., Thomas, R., Shackleton, M., Forrest, N.C., Hartley, L., Robb, L., Grosveld, F.G., van der Wees, J., *et al.* (2007). Gata-3 is an essential regulator of mammary-gland morphogenesis and luminal-cell differentiation. *Nature cell biology* 9, 201-209.
- Barczyk, M., Carracedo, S., and Gullberg, D. (2010). Integrins. *Cell Tissue Res* 339, 269-280.
- Blaas, L., Pucci, F., Messal, H.A., Andersson, A.B., Josue Ruiz, E., Gerling, M., Douagi, I., Spencer-Dene, B., Musch, A., Mitter, R., *et al.* (2016). Lgr6 labels a rare population of mammary gland progenitor cells that are able to originate luminal mammary tumours. *Nature cell biology* 18, 1346-1356.
- Briskin, C., and Ataca, D. (2015). Endocrine hormones and local signals during the development of the mouse mammary gland. *Wiley Interdiscip Rev Dev Biol* 4, 181-195.
- Briskin, C., and O'Malley, B. (2010). Hormone action in the mammary gland. *Cold Spring Harb Perspect Biol* 2, a003178.
- Burute, M., and Thery, M. (2012). Spatial segregation between cell-cell and cell-matrix adhesions. *Curr Opin Cell Biol* 24, 628-636.
- Carr, M.I., and Jones, S.N. (2016). Regulation of the Mdm2-p53 signaling axis in the DNA damage response and tumorigenesis. *Transl Cancer Res* 5, 707-724.
- Chiche, A., Di-Cicco, A., Sesma-Sanz, L., Bresson, L., de la Grange, P., Glukhova, M.A., Faraldo, M.M., and Deugnier, M.A. (2019). p53 controls the plasticity of mammary luminal progenitor cells downstream of Met signaling. *Breast Cancer Res* 21, 13.
- Chiche, A., Moumen, M., Petit, V., Jonkers, J., Medina, D., Deugnier, M.A., Faraldo, M.M., and Glukhova, M.A. (2013). Somatic loss of p53 leads to stem/progenitor cell amplification in both mammary epithelial compartments, basal and luminal. *Stem Cells* 31, 1857-1867.
- De Arcangelis, A., Hamade, H., Alpy, F., Normand, S., Bruyere, E., Lefebvre, O., Mechine-Neuville, A., Siebert, S., Pfister, V., Lepage, P., *et al.* (2017). Hemidesmosome integrity protects the colon against colitis and colorectal cancer. *Gut* 66, 1748-1760.
- de la Grange, P., Dutertre, M., Martin, N., and Auboeuf, D. (2005). FAST DB: a website resource for the study of the expression regulation of human gene products. *Nucleic Acids Res* 33, 4276-4284.
- Di-Cicco, A., Petit, V., Chiche, A., Bresson, L., Romagnoli, M., Orian-Rousseau, V., Vivanco, M., Medina, D., Faraldo, M.M., Glukhova, M.A., *et al.* (2015). Paracrine Met signaling triggers epithelial-mesenchymal transition in mammary luminal progenitors, affecting their fate. *Elife* 4.
- Dobin, A., Davis, C.A., Schlesinger, F., Drenkow, J., Zaleski, C., Jha, S., Batut, P., Chaisson, M., and Gingeras, T.R. (2013). STAR: ultrafast universal RNA-seq aligner. *Bioinformatics* 29, 15-21.
- Elias, S., Morgan, M.A., Bikoff, E.K., and Robertson, E.J. (2017). Long-lived unipotent Blimp1-positive luminal stem cells drive mammary gland organogenesis throughout adult life. *Nat Commun* 8, 1714.
- Ewald, A.J., Brenot, A., Duong, M., Chan, B.S., and Werb, Z. (2008). Collective epithelial migration and cell rearrangements drive mammary branching morphogenesis. *Dev Cell* 14, 570-581.

Faraldo, M.M., Deugnier, M.A., Lukashev, M., Thiery, J.P., and Glukhova, M.A. (1998). Perturbation of beta1-integrin function alters the development of murine mammary gland. *Embo J* 17, 2139-2147.

Faraldo, M.M., Deugnier, M.A., Tlouzeau, S., Thiery, J.P., and Glukhova, M.A. (2002). Perturbation of beta1-integrin function in involuting mammary gland results in premature dedifferentiation of secretory epithelial cells. *Mol Biol Cell* 13, 3521-3531.

Fernandez-Valdivia, R., Mukherjee, A., Ying, Y., Li, J., Paquet, M., DeMayo, F.J., and Lydon, J.P. (2009). The RANKL signaling axis is sufficient to elicit ductal side-branching and alveologenesis in the mammary gland of the virgin mouse. *Dev Biol* 328, 127-139.

Glukhova, M.A., and Streuli, C.H. (2013). How integrins control breast biology. *Curr Opin Cell Biol* 25, 633-641.

Hynes, R.O. (2002). Integrins: bidirectional, allosteric signaling machines. *Cell* 110, 673-687.

Jerry, D.J., Dickinson, E.S., Roberts, A.L., and Said, T.K. (2002). Regulation of apoptosis during mammary involution by the p53 tumor suppressor gene. *J Dairy Sci* 85, 1103-1110.

Jerry, D.J., Kuperwasser, C., Downing, S.R., Pinkas, J., He, C., Dickinson, E., Marconi, S., and Naber, S.P. (1998). Delayed involution of the mammary epithelium in BALB/c-p53null mice. *Oncogene* 17, 2305-2312.

Jonkers, J., Meuwissen, R., van der Gulden, H., Peterse, H., van der Valk, M., and Berns, A. (2001). Synergistic tumor suppressor activity of BRCA2 and p53 in a conditional mouse model for breast cancer. *Nat Genet* 29, 418-425.

Klinowska, T.C., Alexander, C.M., Georges-Labouesse, E., Van der Neut, R., Kreidberg, J.A., Jones, C.J., Sonnenberg, A., and Streuli, C.H. (2001). Epithelial development and differentiation in the mammary gland is not dependent on alpha 3 or alpha 6 integrin subunits. *Dev Biol* 233, 449-467.

Kritikou, E.A., Sharkey, A., Abell, K., Came, P.J., Anderson, E., Clarkson, R.W., and Watson, C.J. (2003). A dual, non-redundant, role for LIF as a regulator of development and STAT3-mediated cell death in mammary gland. *Development* 130, 3459-3468.

Lee, J.L., and Streuli, C.H. (2014). Integrins and epithelial cell polarity. *J Cell Sci* 127, 3217-3225.

Li, N., Zhang, Y., Naylor, M.J., Schatzmann, F., Maurer, F., Wintermantel, T., Schuetz, G., Mueller, U., Streuli, C.H., and Hynes, N.E. (2005). Beta1 integrins regulate mammary gland proliferation and maintain the integrity of mammary alveoli. *Embo J* 24, 1942-1953.

Lim, E., Vaillant, F., Wu, D., Forrest, N.C., Pal, B., Hart, A.H., Asselin-Labat, M.L., Gyorki, D.E., Ward, T., Partanen, A., *et al.* (2009). Aberrant luminal progenitors as the candidate target population for basal tumor development in BRCA1 mutation carriers. *Nat Med* 15, 907-913.

Liu, K., Cheng, L., Flesken-Nikitin, A., Huang, L., Nikitin, A.Y., and Pauli, B.U. (2010). Conditional knockout of fibronectin abrogates mouse mammary gland lobuloalveolar differentiation. *Dev Biol* 346, 11-24.

Love, M.I., Huber, W., and Anders, S. (2014). Moderated estimation of fold change and dispersion for RNA-seq data with DESeq2. *Genome Biol* 15, 550.

Macias, H., and Hinck, L. (2012). Mammary gland development. *Wiley Interdiscip Rev Dev Biol* 1, 533-557.

Margadant, C., Raymond, K., Kreft, M., Sachs, N., Janssen, H., and Sonnenberg, A. (2009). Integrin alpha3beta1 inhibits directional migration and wound re-epithelialization in the skin. *J Cell Sci* 122, 278-288.

Molyneux, G., Geyer, F.C., Magnay, F.A., McCarthy, A., Kendrick, H., Natrajan, R., Mackay, A., Grigoriadis, A., Tutt, A., Ashworth, A., *et al.* (2010). BRCA1 basal-like breast cancers originate from luminal epithelial progenitors and not from basal stem cells. *Cell Stem Cell* 7, 403-417.

Muschler, J., Lochter, A., Roskelley, C.D., Yurchenco, P., and Bissell, M.J. (1999). Division of labor among the alpha6beta4 integrin, beta1 integrins, and an E3 laminin receptor to signal morphogenesis and beta-casein expression in mammary epithelial cells. *Mol Biol Cell* 10, 2817-2828.

Muschler, J., and Streuli, C.H. (2010). Cell-matrix interactions in mammary gland development and breast cancer. *Cold Spring Harb Perspect Biol* 2, a003202.

Naylor, M.J., Li, N., Cheung, J., Lowe, E.T., Lambert, E., Marlow, R., Wang, P., Schatzmann, F., Wintermantel, T., Schuetz, G., *et al.* (2005). Ablation of beta1 integrin in mammary epithelium reveals a key role for integrin in glandular morphogenesis and differentiation. *J Cell Biol* 171, 717-728.

Pullan, S., Wilson, J., Metcalfe, A., Edwards, G.M., Goberdhan, N., Tilly, J., Hickman, J.A., Dive, C., and Streuli, C.H. (1996). Requirement of basement membrane for the suppression of programmed cell death in mammary epithelium. *J Cell Sci* 109 ( Pt 3), 631-642.

Rajkumar, L., Kittrell, F.S., Guzman, R.C., Brown, P.H., Nandi, S., and Medina, D. (2007). Hormone-induced protection of mammary tumorigenesis in genetically engineered mouse models. *Breast Cancer Res* 9, R12.

Ramovs, V., Te Molder, L., and Sonnenberg, A. (2017). The opposing roles of laminin-binding integrins in cancer. *Matrix Biol* 57-58, 213-243.

Raymond, K., Cagnet, S., Kreft, M., Janssen, H., Sonnenberg, A., and Glukhova, M.A. (2011). Control of mammary myoepithelial cell contractile function by alpha3beta1 integrin signalling. *Embo J* 30, 1896-1906.

Raymond, K., Faraldo, M.M., Deugnier, M.A., and Glukhova, M.A. (2012). Integrins in mammary development. *Semin Cell Dev Biol* 23, 599-605.

Rios, A.C., Fu, N.Y., Lindeman, G.J., and Visvader, J.E. (2014). In situ identification of bipotent stem cells in the mammary gland. *Nature* 506, 322-327.

Rodilla, V., Dasti, A., Huyghe, M., Lafkas, D., Laurent, C., Reyat, F., and Fre, S. (2015). Luminal progenitors restrict their lineage potential during mammary gland development. *PLoS Biol* 13, e1002069.

Romagnoli, M., Cagnet, S., Chiche, A., Bresson, L., Baulande, S., de la Grange, P., De Arcangelis, A., Kreft, M., Georges-Labouesse, E., Sonnenberg, A., *et al.* (2019). Deciphering the Mammary Stem Cell Niche: A Role for Laminin-Binding Integrins. *Stem Cell Reports* 12, 831-844.

Sachs, N., Kreft, M., van den Bergh Weerman, M.A., Beynon, A.J., Peters, T.A., Weening, J.J., and Sonnenberg, A. (2006). Kidney failure in mice lacking the tetraspanin CD151. *J Cell Biol* 175, 33-39.

Sargeant, T.J., Lloyd-Lewis, B., Resemann, H.K., Ramos-Montoya, A., Skepper, J., and Watson, C.J. (2014). Stat3 controls cell death during mammary gland involution by regulating uptake of milk fat globules and lysosomal membrane permeabilization. *Nature cell biology* 16, 1057-1068.

Schere-Levy, C., Buggiano, V., Quaglino, A., Gattelli, A., Cirio, M.C., Piazzon, I., Vanzulli, S., and Kordon, E.C. (2003). Leukemia inhibitory factor induces apoptosis of

the mammary epithelial cells and participates in mouse mammary gland involution. *Exp Cell Res* 282, 35-47.

Selbert, S., Bentley, D.J., Melton, D.W., Rannie, D., Lourenco, P., Watson, C.J., and Clarke, A.R. (1998). Efficient BLG-Cre mediated gene deletion in the mammary gland. *Transgenic Res* 7, 387-396.

Shackleton, M., Vaillant, F., Simpson, K.J., Stingl, J., Smyth, G.K., Asselin-Labat, M.L., Wu, L., Lindeman, G.J., and Visvader, J.E. (2006). Generation of a functional mammary gland from a single stem cell. *Nature* 439, 84-88.

Shehata, M., Teschendorff, A., Sharp, G., Novcic, N., Russell, I.A., Avril, S., Prater, M., Eirew, P., Caldas, C., Watson, C.J., *et al.* (2012). Phenotypic and functional characterisation of the luminal cell hierarchy of the mammary gland. *Breast Cancer Res* 14, R134.

Sleeman, K.E., Kendrick, H., Robertson, D., Isacke, C.M., Ashworth, A., and Smalley, M.J. (2007). Dissociation of estrogen receptor expression and in vivo stem cell activity in the mammary gland. *J Cell Biol* 176, 19-26.

Soriano, P. (1999). Generalized lacZ expression with the ROSA26 Cre reporter strain. *Nat Genet* 21, 70-71.

Stingl, J., Eirew, P., Ricketson, I., Shackleton, M., Vaillant, F., Choi, D., Li, H.I., and Eaves, C.J. (2006). Purification and unique properties of mammary epithelial stem cells. *Nature* 439, 993-997.

Streuli, C.H., Schmidhauser, C., Bailey, N., Yurchenco, P., Skubitz, A.P., Roskelley, C., and Bissell, M.J. (1995). Laminin mediates tissue-specific gene expression in mammary epithelia. *J Cell Biol* 129, 591-603.

Taddei, I., Deugnier, M.A., Faraldo, M.M., Petit, V., Bouvard, D., Medina, D., Fassler, R., Thiery, J.P., and Glukhova, M.A. (2008). Beta1 integrin deletion from the basal compartment of the mammary epithelium affects stem cells. *Nat Cell Biol* 10, 716-722.

Teuliere, J., Faraldo, M.M., Deugnier, M.A., Shtutman, M., Ben-Ze'ev, A., Thiery, J.P., and Glukhova, M.A. (2005). Targeted activation of beta-catenin signaling in basal mammary epithelial cells affects mammary development and leads to hyperplasia. *Development* 132, 267-277.

Truchet, S., and Honvo-Houeto, E. (2017). Physiology of milk secretion. *Best Pract Res Clin Endocrinol Metab* 31, 367-384.

Van Keymeulen, A., Fioramonti, M., Centonze, A., Bouvencourt, G., Achouri, Y., and Blanpain, C. (2017). Lineage-Restricted Mammary Stem Cells Sustain the Development, Homeostasis, and Regeneration of the Estrogen Receptor Positive Lineage. *Cell Rep* 20, 1525-1532.

Van Keymeulen, A., Rocha, A.S., Ousset, M., Beck, B., Bouvencourt, G., Rock, J., Sharma, N., Dekoninck, S., and Blanpain, C. (2011). Distinct stem cells contribute to mammary gland development and maintenance. *Nature* 479, 189-193.

Visvader, J.E., and Smith, G.H. (2011). Murine mammary epithelial stem cells: discovery, function, and current status. *Cold Spring Harb Perspect Biol* 3.

Walker, M.R., Amante, J.J., Li, J., Liu, H., Zhu, L.J., Feltri, M.L., Goel, H.L., and Mercurio, A.M. (2020). Alveolar progenitor cells in the mammary gland are dependent on the beta4 integrin. *Dev Biol* 457, 13-19.

Wang, C., Christin, J.R., Oktay, M.H., and Guo, W. (2017). Lineage-Biased Stem Cells Maintain Estrogen-Receptor-Positive and -Negative Mouse Mammary Luminal Lineages. *Cell Rep* 18, 2825-2835.

## FIGURE LEGENDS

### Figure 1. Lack of laminin binding integrins affects mammary alveologenesis and luminal progenitor function in pregnancy.

(A) Immunofluorescence labeling of sections through 15-day-pregnant mammary gland with antibodies against  $\alpha 3$ ,  $\alpha 6$ ,  $\beta 1$  and  $\beta 4$  integrins (green), pankeratin (TK), keratin-8 (K8) and  $\alpha$ -smooth-muscle actin (SMA) (red). Of note, the  $\alpha 3$  and  $\alpha 6$  staining encircling the alveoli reflects untargeted basal cell displaying normal integrin expression. DAPI served to visualize nuclei. Areas within rectangles are shown at 2.5X below each image. Bar, 10  $\mu\text{m}$ .

(B) Dot plot showing separation of luminal (blue shape) and basal (red circle) epithelial cells from 15-day-pregnant mouse mammary glands by flow cytometry. A representative experiment is shown. Most of the luminal cells from  $\alpha 3\alpha 6\text{KO}$  mice are negative for  $\alpha 6$  integrin.

(C) Immunofluorescence labeling of sections through 15-day-pregnant mouse mammary gland with antibodies against  $\alpha 6$  integrin and Progesterone Receptor DAPI served to visualize nuclei. Arrows show cells coexpressing  $\alpha 6$  integrin and PR in the  $\alpha 3\alpha 6\text{KO}$  gland. Bar, 10  $\mu\text{m}$ .

(D) Histograms showing expression of  $\beta 1$  and  $\beta 4$  integrins in luminal cells from 15-day-pregnant mammary glands.

(E) Microphotographs of 15-day-pregnant control and  $\alpha 3\alpha 6\text{KO}$  mouse mammary glands. Left, fragments of glands stained with Carmine in whole-mount (bar, 0.8 mm); right, Hematoxylin/Eosin (H&E) staining of gland sections (bar, 40  $\mu\text{m}$ ). The graph shows quantification of the relative alveolar density, the values shown are means $\pm$ SD obtained from 3 animals per genotype. \*  $p = 0.004$ .

(F) Mammosphere formation by luminal cells sorted from 15-day-pregnant mouse mammary glands. Left, representative microphotographs (bar, 750  $\mu\text{m}$ ). The graph shows quantification of mammosphere number, values shown are means $\pm$ SD obtained from 4 independent experiments. \*  $p = 0.03$ . Values obtained for control cells were set as 1 in each experiment.

(G) RT-qPCR analysis of milk protein gene expression in freshly sorted luminal cells from 15-day-pregnant mouse mammary glands. The values shown are means $\pm$ SD obtained from 4 independent experiments. \*  $p = 0.03$  for *Wap*; 0.003 for *Lalba*; 0.027 for *Csn2*.

(H) RT-qPCR analysis of gene expression in freshly sorted luminal cells from 15-day-pregnant mouse mammary glands. The values shown are means $\pm$ SD obtained from three independent experiments.  $p < 0.05$  for all genes analyzed.

**Figure 2. The deletion of LN-binding integrins affects luminal progenitor activation in response to ovarian hormones.**

(A) Microphotographs of E/P-stimulated control and  $\alpha 3\alpha 6$ KO mouse mammary glands. Left, fragments of glands stained with Carmine in whole-mount (bar, 400  $\mu$ m); right, H&E staining of gland sections (bar, 40  $\mu$ m). The graph shows quantification of the relative alveolar density, the values shown are means $\pm$ SD obtained from 4 independent experiments. \*  $p = 0.026$ .

(B) Immunofluorescence staining of control and  $\alpha 3\alpha 6$ KO mouse mammary gland sections with antibodies against Ki67 and  $\alpha$ SMA. The graph shows quantification of Ki67 positive cells, the values shown are means $\pm$ SD obtained from 3 animals per group. \*  $p = 0.017$ .

(C) Dot plot showing separation of luminal (L) and basal (B) epithelial cells from E/P-stimulated mammary glands by flow cytometry. In  $\alpha 3\alpha 6$ KO mice, a fraction of the luminal cell population is devoid of  $\alpha 6$  integrin expression.

(D) Histograms showing expression of  $\alpha 6$  integrin in mature luminal cells (L-ICAM $^-$ ) and luminal progenitors (L-ICAM $^+$ ) from E/P-stimulated mammary glands by flow cytometry. L-ICAM $^-$  and L-ICAM $^+$  populations were separated as described in Fig. S1A. The graph shows the percentage of  $\alpha 6$  integrin negative luminal cells in both luminal populations, presented as means $\pm$ SD obtained from 5 independent experiments.

(E) Mammosphere formation capacity of luminal progenitor cells isolated from E/P-stimulated mammary glands. The graph shows means $\pm$ SD;  $n = 3$  ( $\alpha 3$ KO and  $\alpha 6$ KO) or  $n = 5$  (Ctrl and  $\alpha 3\alpha 6$ KO) independent experiments; \*  $p = 0.0003$ .

(F) RT-qPCR analysis of gene expression in freshly sorted luminal progenitor cells from E/P-stimulated mammary glands. The graph shows means $\pm$ SD obtained from three independent experiments. \*  $p = 0.007$  for *Wap*; 0.003 for *Csn2*; 0.009 for *Elf5*.

**Figure 3. The deletion of LN-binding integrins leads to basal cell shape changes but does not affect early lactation.**

(A) H&E staining of sections through 2-day-lactating mammary glands of control and  $\alpha3\alpha6$ KO females. Bar, 150  $\mu\text{m}$ .

(B) RT-qPCR analysis of milk protein gene expression in freshly isolated luminal cells sorted from 2-day-lactating mammary glands. The graph shows means $\pm$ SD obtained from 4 independent experiments; n.s., not statistically significant.

(C) Weight of the pups fed by control or  $\alpha3\alpha6$ KO females for 2 days. The litters from 6 females per genotype were analyzed; n.s., not statistically significant.

(D) Immunofluorescence labeling of sections through 2-day-lactating mouse mammary glands with antibodies against  $\alpha6$  integrin and  $\alpha$ -smooth-muscle actin (SMA). DAPI served to visualize nuclei. Confocal images are shown. Bar, 62  $\mu\text{m}$  (upper panels), 25  $\mu\text{m}$  (lower panels).

(E) Diagram showing the percentage of the alveolar surface covered by basal SMA+ cells. The graph shows means $\pm$ SD obtained from three control and three  $\alpha3\alpha6$ KO mammary glands at 2 days of lactation; at least 8 alveoli were quantified for each animal. \*  $p = 0.0001$ .

(F) Diagram showing branch cell width of alveolar basal. The graph shows means $\pm$ SD obtained from three control and three  $\alpha3\alpha6$ KO mammary glands at 2 days of lactation; at least 20 cells were quantified for each animal. \*  $p = 0.0004$ .

(G) Heatmap based on RNA-seq analysis showing genes differentially expressed in freshly isolated control and  $\alpha3\alpha6$ KO mammary basal cells from 2-day-lactating mice. Four control and three  $\alpha3\alpha6$ KO females were analyzed.

**Figure 4. The deletion of LN-binding integrins disturbs luminal cell baso-apical polarization and leads to unscheduled involution**

(A) H&E staining of sections through 21-day-lactating mouse mammary glands from control,  $\alpha3$ KO,  $\alpha6$ KO and  $\alpha3\alpha6$ KO females. Bar, 150  $\mu\text{m}$ .

(B) Weight of the pups fed by control,  $\alpha3$ KO,  $\alpha6$ KO or  $\alpha3\alpha6$ KO females after 7, 14 and 21 days of lactation. The litters from 4 females per genotype were analyzed; \*  $p = 0.04$  (lactation day 14) and 0.006 (lactation day 21) for  $\alpha3\alpha6$ KO litters, and 0.003 (lactation day 21) for  $\alpha6$ KO litters.

(C) RT-qPCR analysis of milk protein gene expression in 21-day-lactating mouse mammary glands. The graph shows means $\pm$ SD; 4 females per genotype were analyzed; \*  $p = 0.012$  for *Csn2*; 0.05 for *Wap* ; 0.003 for *Lalba*.

(D) H&E staining of sections through 14-day-lactating mouse mammary glands. Bar, 30  $\mu$ m.

(E) Immunofluorescence labeling of sections through 14-day-lactating mouse mammary gland with an antibody against GM130. DAPI served to visualize nuclei. The basement membrane (B.M.) is indicated by a dotted line. The arrow shows a cell with normal apical localization of GM130, asterisks mark cells with aberrant basal GM130 localization. Bar, 10  $\mu$ m. The graph shows means $\pm$ SD, three females per genotype were analyzed, and a minimum of 250 cells per sample were counted; \*  $p = 0.002$ .

(F), (G) Immunofluorescence labeling of sections through 14-day-lactating mouse mammary gland with an antibody against GM130 and Par3 (F) and antibodies against the Laminin-5 and E-cadherin (G). DAPI served to visualize nuclei. Asterisks mark cells with aberrant Par3 and E-cadherin localization. Bar, 15  $\mu$ m.

(H) TUNEL assay performed with sections through 21-day-lactating mammary glands from control and  $\alpha 3\alpha 6$ KO females. Methyl green was used as counterstaining. Arrowheads indicate TUNEL-positive cells. Bar, 50  $\mu$ m. The values presented in the graph show means $\pm$ SD, 4 females per genotype were analyzed, \*  $p = 0.05$ .

(I) RT-qPCR analysis of *Lif* expression in 21-day-lactating mouse mammary glands. The values presented in the graph show means $\pm$ SD, 4 females per genotype were analyzed, \*  $p = 0.005$ .

**Figure 5. Genetic p53 suppression restores growth but not differentiation in mammary luminal cells depleted of LN-binding integrins**

(A) Heatmap based on microarray analysis of freshly sorted luminal progenitor cells isolated from 15-day-pregnant control and  $\alpha 3\alpha 6$ KO mammary glands.

(B) RT-qPCR analysis of *Cdkn1a* and *Mdm2* gene expression in mammospheres formed by luminal progenitor cells from 15-day-pregnant control and  $\alpha 3\alpha 6$ KO mammary glands. The graph shows means $\pm$ SD obtained in 4 independent experiments; \*  $p = 0.025$  for *Cdkn1a* and 0.04 for *Mdm2*.



(C) Microphotographs of mammary glands from control and  $\alpha3\alpha6p53KO$  females stimulated with ovarian hormones (E/P). Left, whole mount carmine staining, right, H&E staining. Bar, 400  $\mu\text{m}$  (left) and 40  $\mu\text{m}$  (right). The graph shows quantification of the relative alveolar density, presented as means $\pm$ SD obtained from three independent experiments.

(D) Immunofluorescence labeling of sections through mammospheres formed by mammary luminal progenitors sorted from E/P-stimulated control and  $\alpha3\alpha6p53KO$  females with antibodies against K8 and  $\alpha6$  integrin. The graph shows means $\pm$ SD obtained from three independent experiments.

(E) RT-qPCR analysis of milk protein gene expression in freshly isolated mammary luminal progenitors sorted from E/P-stimulated control and  $\alpha3\alpha6p53KO$  females. The graph shows means $\pm$ SD obtained from three independent experiments. \*  $p = 0.006$  for *Csn2*; 0.03 for *Wap*.

(F) H&E staining of sections through 14-day-lactating mammary glands Bar, 90  $\mu\text{m}$ .

(G) Immunofluorescence labeling of sections through 14-day-lactating mouse mammary gland with an antibody against GM130. DAPI served to visualize nuclei. The arrow indicates normal apical localization of GM130 and asterisk, aberrant basal localization. Bar, 10  $\mu\text{m}$ . The values presented in the graph show the means $\pm$ SD, three females per genotype were analyzed; at least 250 cells per sample were counted; \*  $p = 0.003$ .

(H) Weight of the pups fed by control or  $\alpha3\alpha6p53KO$  females after 7, 14 and 21 days of lactation. The litters (7-8 pups) from four females per genotype were analyzed; \*  $p = 0.008$  (lactation day 14) and 0.016 (lactation day 21).

(I) RT-qPCR analysis of milk protein gene expression in 21-day-lactating mammary glands from control and  $\alpha3\alpha6p53KO$  females. The values presented in the graph show the means $\pm$ SD, 4 females per genotype were analyzed, \*  $p = 0.11$  for *Csn2*; 0.004 for *Lalba*; 0.045 for *Wap*.

### **Figure 6. Activation of a Rho/MyosinIII/p53 pathway following depletion of LN-binding integrins in mammary luminal progenitors**

(A) Mammospheres formed by luminal progenitor cells following adenoCre-mediated integrin depletion and counted after 12 days of culture. Left, representative

microphotographs of mammospheres formed by control,  $\alpha3\alpha6$ KO and  $\alpha3\alpha6p53$ KO luminal progenitor cells (bar, 400  $\mu$ m). The graph shows means $\pm$ SD obtained in three independent experiments. For  $\alpha3\alpha6$ KO versus control,  $p = 0.014$ ; for  $\alpha3\alpha6$ KO versus  $\alpha3\alpha6p53$ KO,  $p = 0.02$ .

(B) RT-qPCR analysis of *Cdkn1a* gene expression in cells obtained from mammospheres formed by control,  $\alpha3\alpha6$ KO and  $\alpha3\alpha6p53$ KO luminal progenitor cells. The graph shows means $\pm$ SD obtained in three independent experiments. For  $\alpha3\alpha6$ KO versus control,  $p = 0.034$ ; for  $\alpha3\alpha6$ KO versus  $\alpha3\alpha6p53$ KO,  $p = 0.001$ .

(C) Mammospheres formation by control,  $\alpha3\alpha6$ KO and  $\alpha3\alpha6p53$ KO luminal progenitor cells in the presence of Y27632 or Blebbistatin. The graph shows means $\pm$ SD obtained in three independent experiments. For control mammospheres,  $p = 0.045$  for Y27632-treated cells compared to non-treated cells,  $p = 0.05$  for Blebbistatin-treated cells compared to non-treated cells. For  $\alpha3\alpha6$ KO mammospheres,  $p = 0.033$  for Y27632-treated cells compared to non-treated cells,  $p = 0.024$  for Blebbistatin-treated cells compared to non-treated cells.

(D) RT-qPCR analysis of *Cdkn1a* gene expression in cells obtained from mammospheres formed by luminal progenitor cells in the presence of Y27632 or Blebbistatin. The graph shows means $\pm$ SD obtained in three independent experiments. For control mammospheres,  $p = 0.005$  for Y27632-treated cells compared to non-treated cells,  $p = 0.01$  for Blebbistatin-treated cells compared to non-treated cells. For  $\alpha3\alpha6$ KO mammospheres,  $p = 0.006$  for Y27632-treated cells compared to non-treated cells,  $p = 0.023$  for Blebbistatin-treated cells compared to non-treated cells.

(E) Western blotting analysis of p53 and MDM2 protein levels in extracts of mammosphere formed by control,  $\alpha3\alpha6$ KO and  $\alpha3\alpha6p53$ KO luminal cells. GAPDH was used as a loading control. A representative experiment is shown.

Values obtained for control cells were set as 1 in each experiment. Through the whole figure: Y, Y27632, B, Blebbistatin.

Figure 1

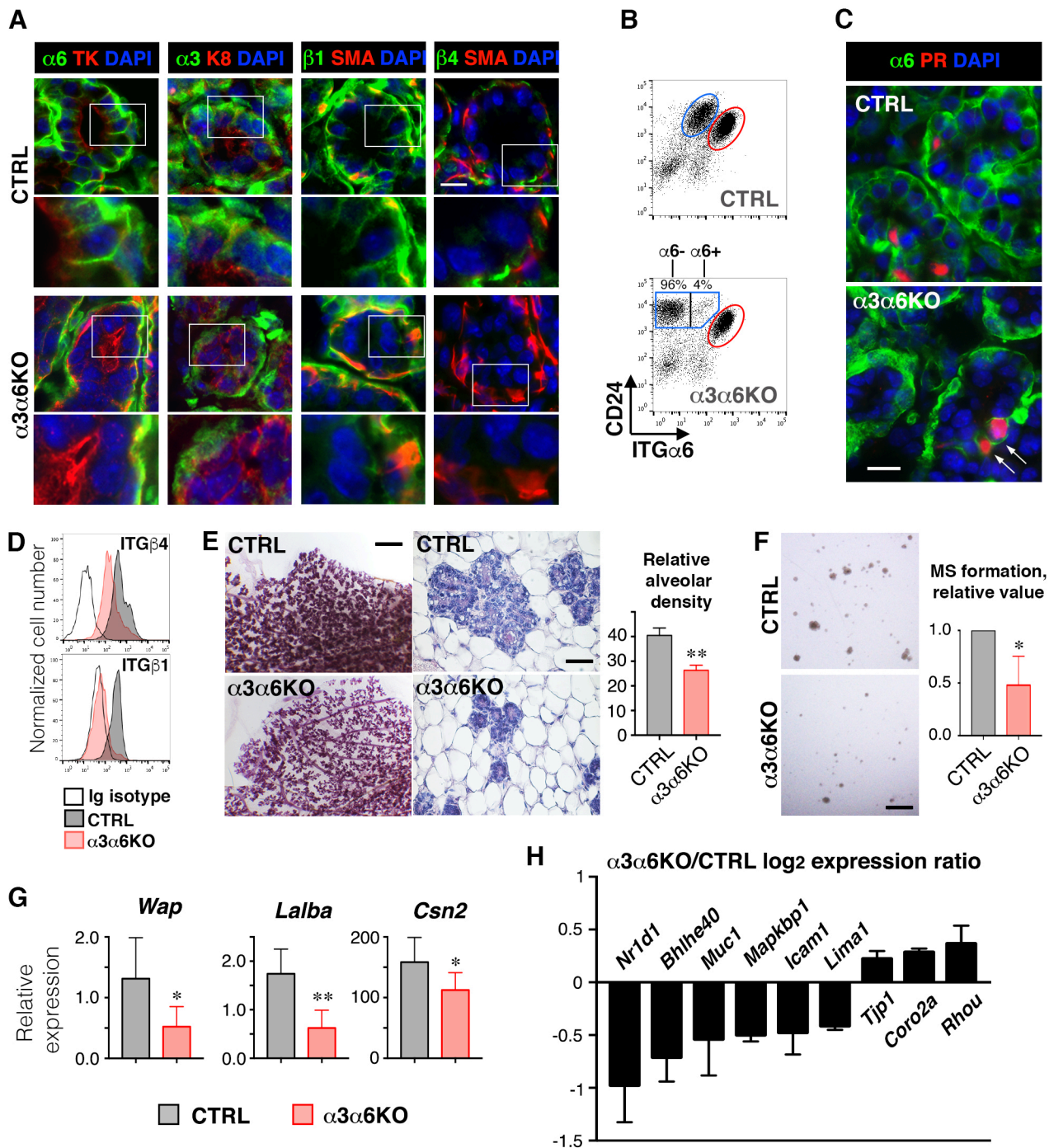


**Figure 2**

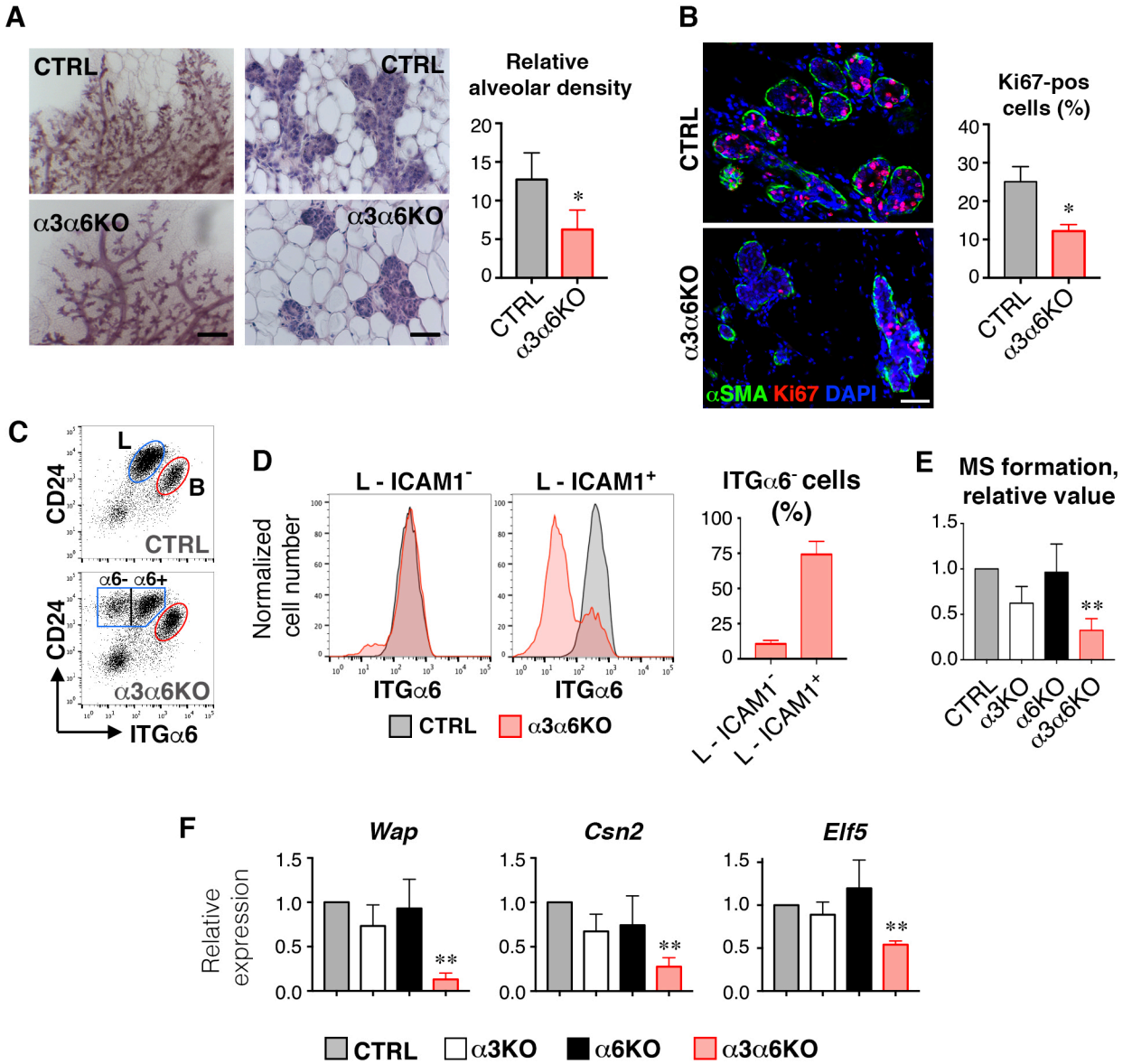


**Figure 3**

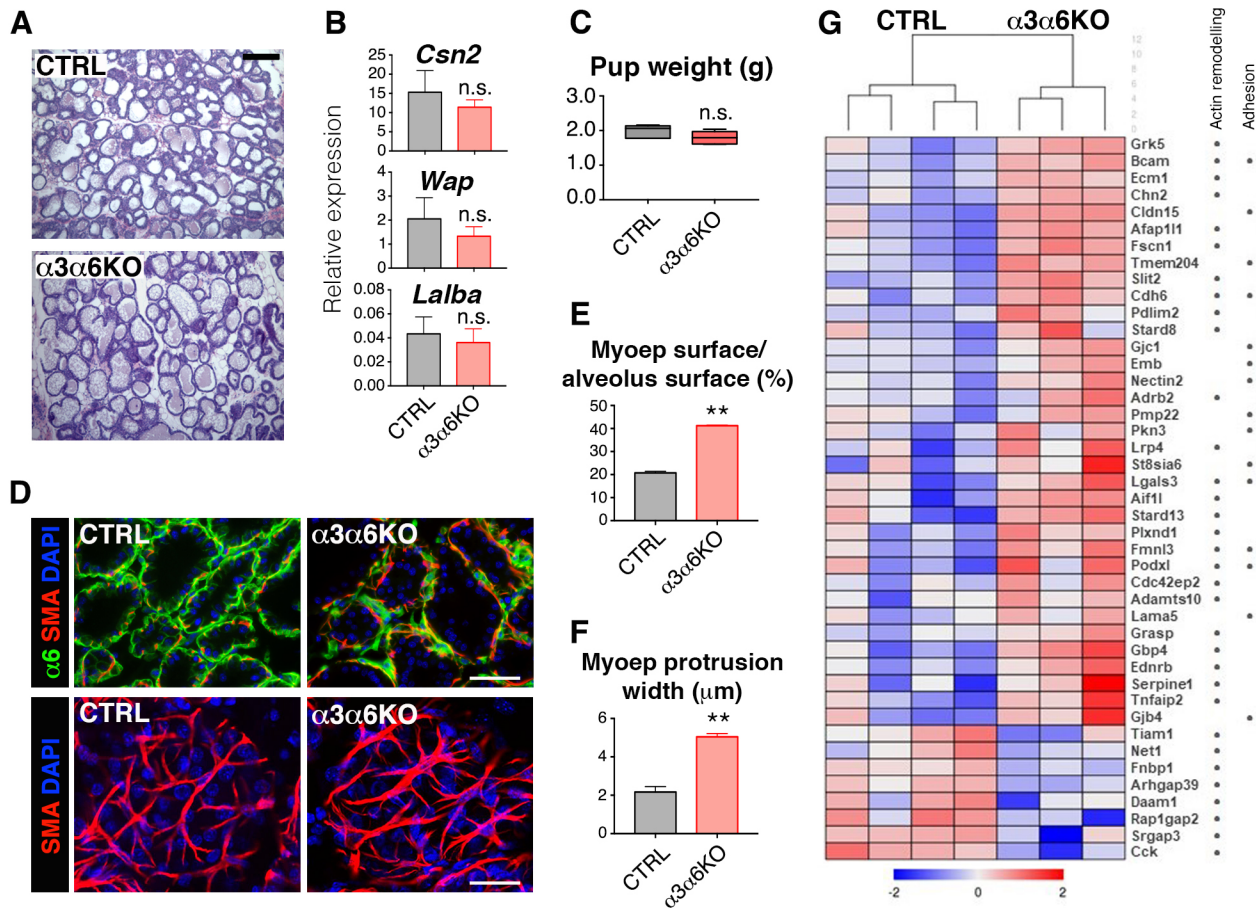




**Figure 4**

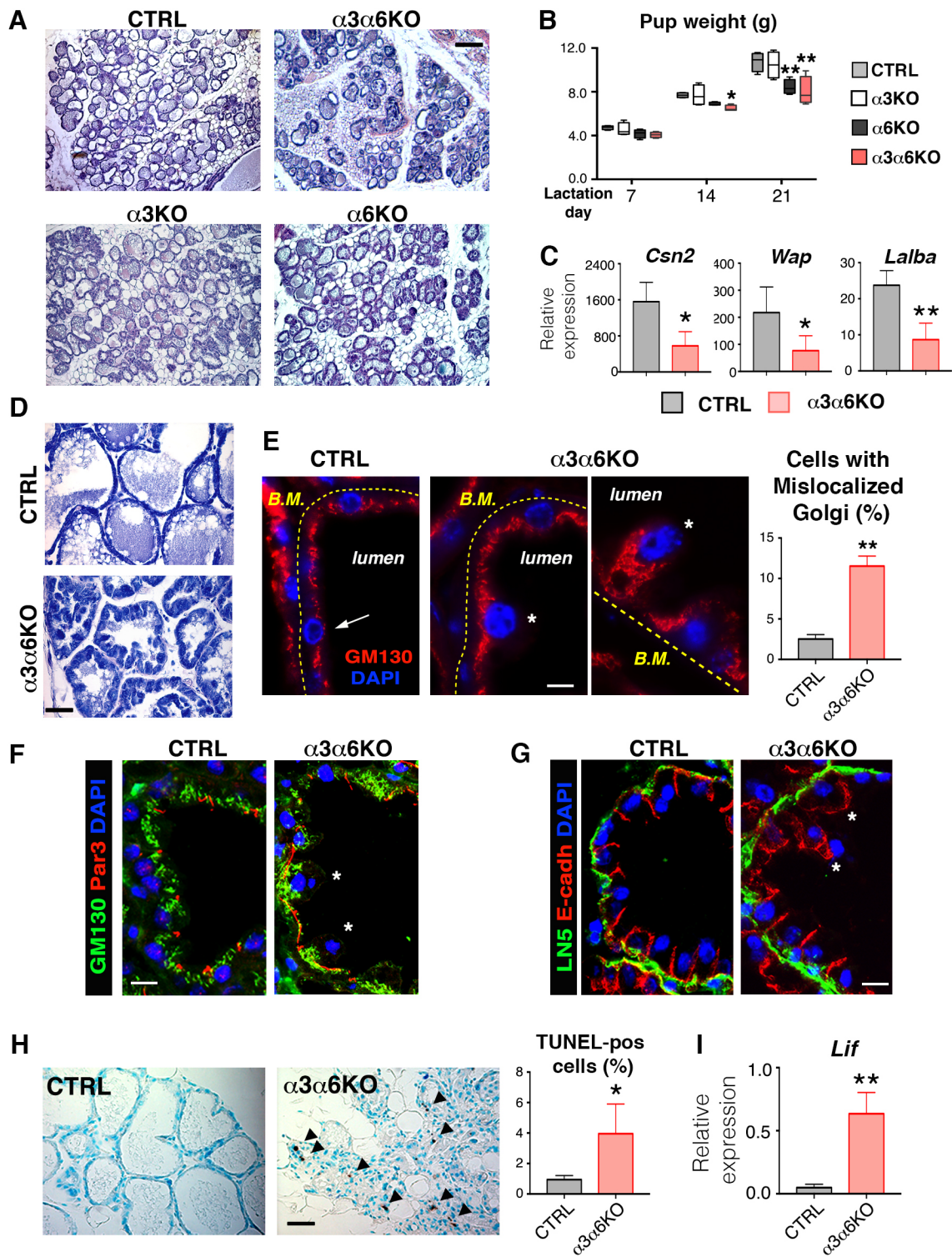


**Figure 5**

